VILNIUS UNIVERSITY

LIFE SCIENCES CENTER

Goda Grigorianaitė

Development of a Microfluidic System for Cultivating and Studying Microbial Biofilms Under Controlled Flow Conditions

Master's Thesis

Molecular Biotechnology study program

Thesis supervisor

Dr. Wanessa Melo

Consultant

Adei Abouhagger

Thesis completed at

Department of Functional Materials and Electronics,
FTMC (Center for Physical Sciences and Technology)

Vilnius 2024

Table of Contents

ABBREVIATIONS

BHI – brain heart infusion broth

CFU – colony–forming units

CLSM – confocal laser scanning microscopy

COC – cyclo–olefin copolymer

Escherichia coli – E. coli

IPA – isopropanol

OSTE – off–stoichiometry thiol–ene

PBS – phosphate–buffered saline

PDMS – polydimethylsiloxane

PMBF – polymicrobial biofilm

Pseudomonas aeruginosa – P. aeruginosa

Staphylococcus aureus – S. aureus

WSS – wall shear stress

INTRODUCTION

Bacterial biofilms can cause a broad spectrum of serious infections and are associated with chronic, non–healing infections (Fleming & Rumbaugh, 2017). According to the National Institutes of Health (NIH), approximately 65% and 80% of microbial and chronic infections are associated with biofilm formation (Jamal et al., 2018). Additionally, increasing numbers of antibiotic–resistant bacteria make the investigation of biofilm formation and ways to inhibit it increasingly urgent. To better understand how biofilms can be treated, various *in vitro* study models have been created. These study methods are divided into two main groups: static and dynamic (Alcàcer–Almansa et al., 2023). Static methods are widely used in microbiology labs due to their low costs and easy–to–use approach. However, these methods have several disadvantages, such as inability to mimic the natural environment, lack of consistent flow and nutrients, and build–up of metabolic waste, which can inhibit biofilm formation and growth (Cleaver & Garnett, 2023). In contrast, dynamic methods, these issues are recognised, with microfluidic chips being one of the newly emerged solutions.

A microfluidic chip is a platform in which flow is controlled at a micrometric scale (Son et al., 2015). Microfluidic chips are recognised as a promising platform for studying bacterial biofilms, because they provide a closed system in which the flow and environment are controlled and can be manipulated according to the experimental requirements. Apart from that, materials used in the microfluidic chip fabrication are often transparent, allowing for the analysis of the grown biofilms by using high–throughput analysis systems such as confocal scanning microscopy (Kim et al., 2012). Microchips require less materials and minimize the risk of human errors compared to traditional bacterial biofilm cultivation methods. Also, their compact design simplifies the disinfection process, making it a preferable platform for studying microbial biofilms in clinical settings.

Aim – To develop a microfluidic chip for microbial biofilm investigation.

Research tasks:

1. To fabricate a microfluidic chip for biofilm cultivation and investigation.
2. To compare static (well plates) *versus* dynamic (microfluidic system) biofilm cultivation methods.
3. To assess the reliability of the fabricated microfluidic chip to analyse antimicrobial treatment efficacy to grown microbial biofilms.
4. To grow and analyze polymicrobial biofilm formation in the microfluidic system.

1. LITERATURE REVIEW

1.1. Biofilms and their importance in the medical field

Biofilms are a cluster of microorganisms that produce the extracellular polymeric substance (EPS) in which they are encapsulated (Schulze et al., 2021). According to The National Institutes of Health (NIH), approximately 65% and 80% of microbial and chronic infections are affiliated with biofilm formation (Jamal et al., 2018). Bacterial biofilms can cause a broad spectrum of serious infections and are associated with chronic, non–healing infections (Fleming & Rumbaugh, 2017). Additionally, increasing numbers of antibiotic resistance bacteria make the investigation of biofilm formation and ways how to inhibit it increasingly urgent. The biofilm formation has five main phases: attachment to the surface, irreversible attachment, maturation I (microcolony formation), maturation II, and the last one–dispersion (**Figure 1.1.**) (Chandki et al., 2011). The first phase of biofilm formation starts with free–floating bacteria after encounter with any biotic or abiotic surface. The initial, reversible attachment begins with the help of physical forces or bacteria`s flagella and or pili (Marić & Vraneš, 2007). The level of bacteria`s attachment to the surface depends on temperature, surface material composition, pressure, and even bacteria's surface properties (Zheng et al., 2021). The physical forces such as van der Waals forces, electrostatic and steric interactions also play an essential role in bacterial adhesion (Gupta et al., 2016). In the second phase of biofilm formation, some of the bacteria attached to the surface become irreversibly adhered. These microorganisms form an extracellular polymeric matrix and multiply, forming cell–cell adhesion (Sharma et al., 2023). The third, or maturation I stage, is when microcolony formation and Quorum Sensing production intensifies. Using Quorum Sensing, bacteria communicate with each other by chemical signals. They regulate their cellular functions according to the environment and nutrient availability. During this process, they exchange genetic material, which helps to sync the synthesis of different metabolites (Preda & Săndulescu, 2019). The next biofilm formation stage is maturation II, during which the biofilm grows, and the thickness can reach almost 100 μm. Maturation II is followed by the last stage–dispersion of biofilm. After the biofilm disperses, it colonizes new surfaces, thus spreading the infection.

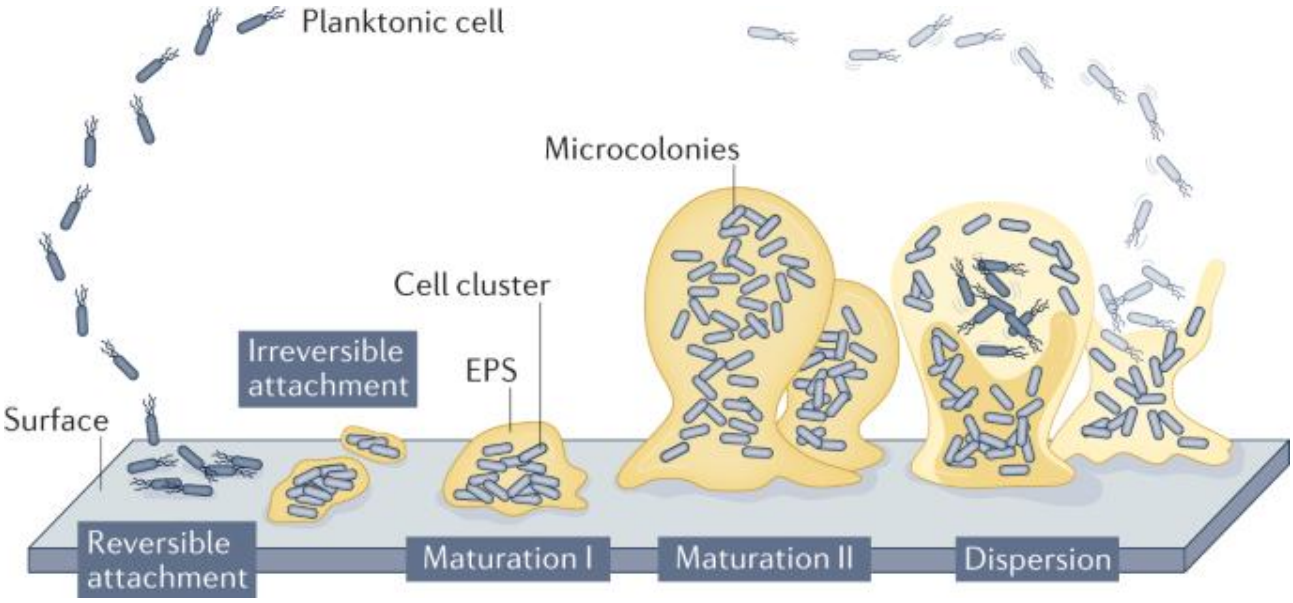

Figure 1.1. Biofilm formation stages (Sauer et al., 2022).

1.2. Polymicrobial biofilm

Polymicrobial biofilms (PMBF) are described as a group, consisting of two or more different microorganisms, such as bacteria, and fungi, which are embedded in EPS matrix and live in a coordinated manner (Anju et al., 2022). In the natural environment, microbes rarely exist without coaggregation, increasing the importance of studying these interactions. Cooperation between different microorganisms and the formation of PMBF enhances survival rates and adaptation to external stresses, therefore, many infections are caused by several interacting bacteria and often result in chronic and recurring diseases, some of the diseases caused by PMBFs are presented in **Figure 1.2**.

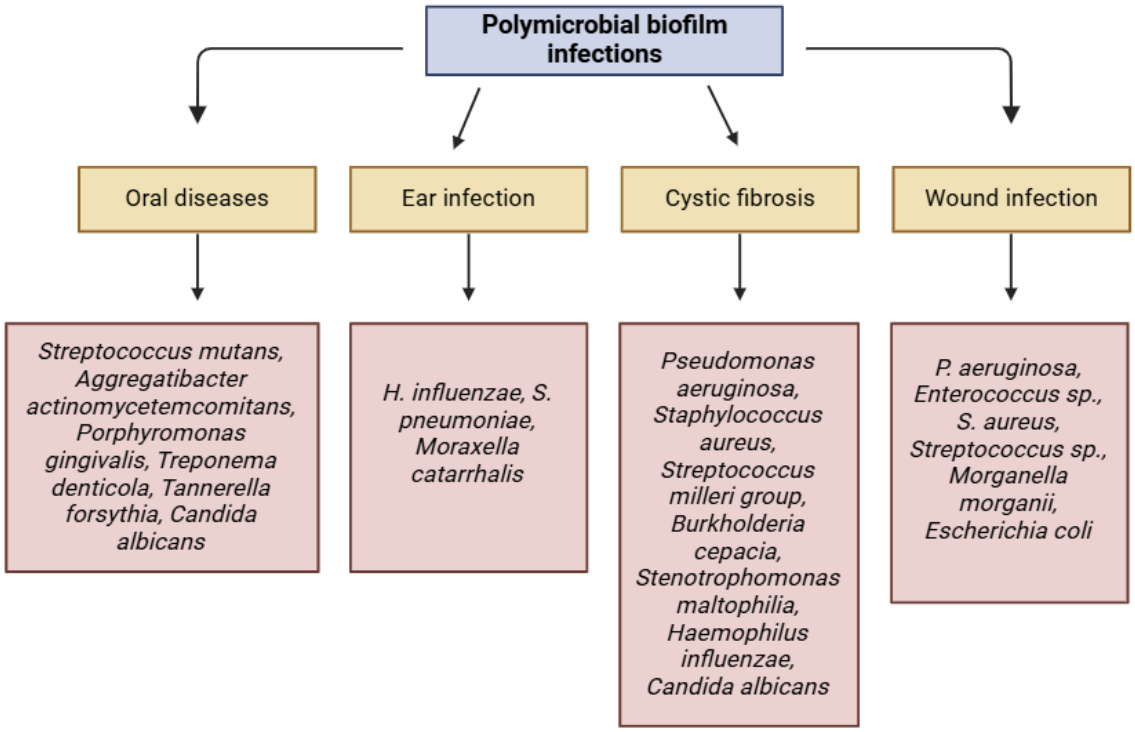

Figure 1.2. Infections associated with different bacteria polymicrobial interactions. The figure shows which bacterial and fungal formed PMBFs can cause chronic infections. The figure was prepared using biorender.com.

However, PMBF brings several advantages to microorganisms, such as increased suppression against the immune system, increased drug resistance, stress tolerance, and virulence (Dhiman et al., 2024). For example, H_2O_2 is known to cause oxidative stress, which negatively affects microorganisms by generating free radicals, including *Streptococcus mutants* and *Candida albicans*. It was observed that in PMBFs consisting of these two microorganisms, stress tolerance was enhanced because genes responsible for stress response in both species were upregulated, increasing the chances of PMBF survival compared to monomicrobial biofilms (Lobo et al., 2019). PMBFs increase the microorganisms' resistance to antimicrobial treatment by hindering the diffusion of these drugs into the biofilm. The efficacy of vancomycin, an antibiotic that is often used against *S. aureus*, was tested in PMBFs consisting of *C. albicans* and *Staphylococcus aureus* (*S. aureus*) microorganisms. In *S. aureus* monomicrobial biofilm vancomycin reached the base level of the biofilm. However, in the mentioned PMBFs antibiotics had almost zero effect, proving that PMBFs have increased antibiotic resistance (Kong et al., 2016). Apart from that, microorganisms in PMBFs increase their chances of survival by coordinating their gene expression and production of virulence factors according to the environment. These factors are small molecules needed for bacteria to cause infection in eucaryotic organisms (Abedon et al., 2009). Elastase is one of the most common virulence factors encoded by LasB (*Pseudomonas aeruginosa* elastase gene), which hydrolyses elastin in host connective tissues and damages them (Keown et al., 2020). When PLMBFs are formed, the

production of elastase increases, causing more severe consequences to the host, making the treatment more difficult for several reasons (Smith et al., 2015). Therefore, there is an increasing need to study PMBFs and the development of more effective treatments against them.

S. aureus and *Pseudomonas aeruginosa (P. aeruginosa)* are the most common pathogens that form biofilms, causing challenging treatment. Therefore, they are the most studied strains of bacteria. *S. aureus* is known to cause pneumonia, osteomyelitis, and endocarditis and can cause several tissue or skin infections (Tong et al., 2015). On the other hand, *P. aeruginosa* can cause chronic or acute infections in patients with burns, sepsis, cystic fibrosis, etc. Also, infections caused by *P. aeruginosa* are complicated to treat because of their high antibacterial resistance and high mutation rate (Qin et al., 2022). Both mentioned bacteria form biofilms, causing a lot of difficulties in treating the infection. However, these bacteria can cooperate and form a polymicrobial biofilm, which is highly pathogenic. *S. aureus* and *P. aeruginosa* are the most commonly encountered bacteria in biofilms–affected chronic wounds. During polymicrobial biofilm formation, *S. aureus* usually attaches first to the surface and starts the biofilm formation, which promotes the increased aggregation of *P. aeruginosa* (Alves et al., 2018). After the first stage of biofilm formation, follow all the usual steps. However, the dynamics inside the polymicrobial biofilm can be competitive, and *P. aeruginosa* can produce antimicrobial compounds and enzymes that could negatively affect *S. aureus* (Alves et al., 2018). This polymicrobial biofilm can cause difficulties in treating chronic wounds and cystic fibrosis while the resistance to the immune system and antibiotics increases (Camus et al., 2022).

Escherichia coli (E. coli) is a widely known bacterial species that is often involved in diseases caused by biofilm formation. Most commonly, *E. coli* biofilm causes urinary tract infections (UTIs), with high chances of relapse (Ballén et al., 2022). Apart from that, *S. aureus* tends to form polymicrobial biofilms with *E. coli*, causing more severe UTIs. The highest rates of UTIs caused by *E. coli* and *S. aureus* were associated with patients who had urinary catheters, where biofilms form in the urinary tract or on catheters (Park et al., 2023). During polymicrobial biofilm formation, *S. aureus* transfers antibiotic resistance genes to *E. coli*, resulting in increased antibiotic resistance (Margarida Pereira et al., 2012).

1.3. Strategies inhibiting biofilm formation

After reviewing all the stages of biofilm formation, the first stage holds the greatest significance in preventing biofilm development. It represents the highest risk and marks the onset of infection. As a result, prevention efforts primarily focus on this initial stage. However, existing methods to prevent infection are not always reliable. For instance, to inhibit bacterial attachment, devices or wound dressings coated with antibiotic–eluting solutions are employed. Unfortunately, these approaches can impair the functionality of the device and contribute to the accelerated emergence of antibiotic–resistant bacteria (Ma et al., 2022). Another option is coating medical devices with antibacterial

materials or solutions. However, often, the use of such an option could result in decreased efficacy and even accumulation of dead cells on the surface. Therefore, it is important that the surface also possess antifouling properties, minimizing the accumulation of cell debris (Wei et al., 2017). Ideally, such applications should also prevent biofilm formation. It was observed that bacterial adhesion and biofilm formation could be prevented by creating a surface using quercetin molecules derived from plant flavonoids, together with an antifouling polymer. The surface adhesion using 2–hydroxyethyl methacrylate was inhibited in an acidic environment as response quercetin molecules were released. This resulted in the degradation of the biofilm structure and disruption of quorum sensing (Zou et al., 2021).

1.4. Analysis of biofilms

1.4.1. Methods to analyse biofilms *in vitro*

As concern for biofilm infections increases every year, it's crucial to study their formation and possible treatment methods. To better understand how biofilms can be treated, various *in vitro* study models have been created. These study methods are divided into two main groups: static and dynamic (Alcàcer–Almansa et al., 2023).

Static methods are among the most popular because they are user–friendly, have low contamination rates, and are low–cost (Cattò & Cappitelli, 2019). The microtitre plate assay is the best example of a static biofilm study, during which biofilms form on the bottom of a microtitre plate and later are stained, usually with crystal violet, for biomass analysis (O'Toole, 2011). However, this method cannot replicate the natural biofilm environment as it's not exposed to the sheer forces that biofilms encounter in the *in vivo* environment, such as the gut or urinary tract. Also, as there is no consistent flow, there could be a lack of nutrients and a build–up of bioproducts, which could inhibit biofilm growth and maturation (Cleaver & Garnett, 2023).

Dynamic methods, different from static ones, create a stream with which nutrients and waste products are continuously flowing. Visualisation of dynamic methods is presented in **Figure 1.4.1**. Several dynamic systems are currently used for biofilm studies, such as modified Robbins devices (MRD), drip flow reactors (DFR), rotary disk reactor and microfluidic devices (Azeredo et al., 2017). MRD flow–based system that has a square channel pipe with removable sampling ports, with microscopic slides on which biofilm forms under consistent parallel nutrient flow, where hydrodynamic conditions are controlled (McCoy et al., 1981). MRD enables analysis of biofilm growth, structure, and response to environmental changes, such as reactions to antibiotics and different material surfaces (Manz et al., 1993; Teodósio et al., 2011). DFR is similar to the MRD and also uses microscopic slides to grow biofilm. The system consists of four parallel chambers in which microscopic slides are placed. Each chamber has vented lids and gauge needles are used to serve growth media to the chamber through lid septum (Schwartz et al., 2010). DFRs are commonly used

to mimic the surface of medical devices and test their antimicrobial properties to assess disinfection strategies against biofilm formation (Buckingham–Meyer et al., 2007). Rotary disk reactor consists of a central spinning disk, attached to the magnet, that is responsible for creating rotational speed and helps to create similar sheer stress to the samples. The central spinning desk can hold several microscopic slides (Schwartz et al., 2010). This method is used for biofilm resistance analysis and for developing assays for biofilm formation control (Coenye & Nelis, 2010). Having in mind all the mentioned methods microfluidics is known as a novel dynamic analysis tool for studying biofilms.

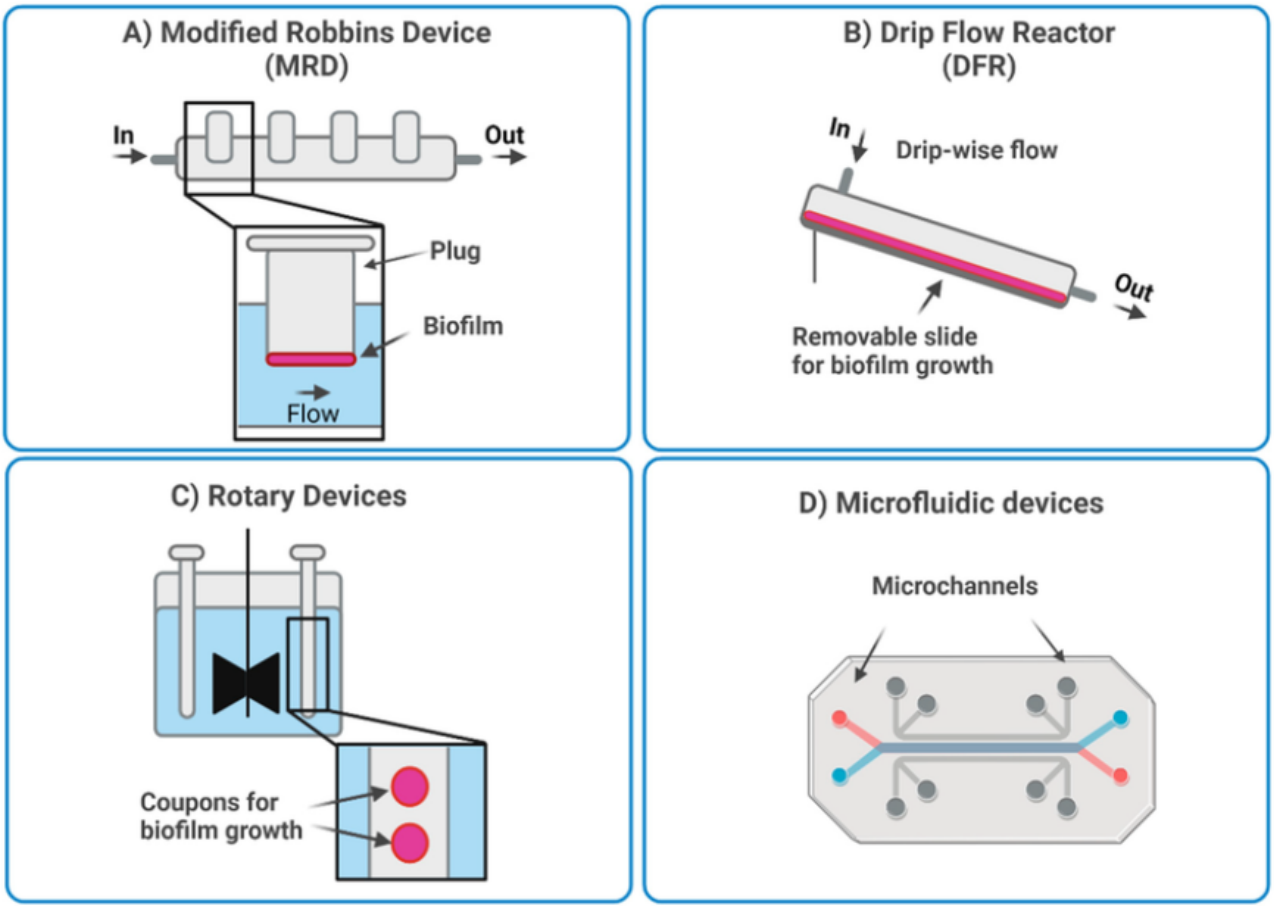

Figure 1.4.1. Visualisation of different dynamic biofilm analysis methods. A – modified Robbins device (MRD), B – drip flow reactor (DFR), C – rotary devices, and D – microfluidic devices (Crivello et al., 2023).

1.4.2. Microfluidic chips for biofilm study

Flow is an integral part of every living organism, enabling the movement of nutrients and waste. In the human body, flow is present in various parts, such as the urinary tract, vasculature, and the gut, where bacteria can all colonize. Flow is recognized as a crucial factor for biofilm formation and growth, starting from the early stages, such as adhesion. The impact of flow on biofilm formation is shown in **Figure 1.4.2**.

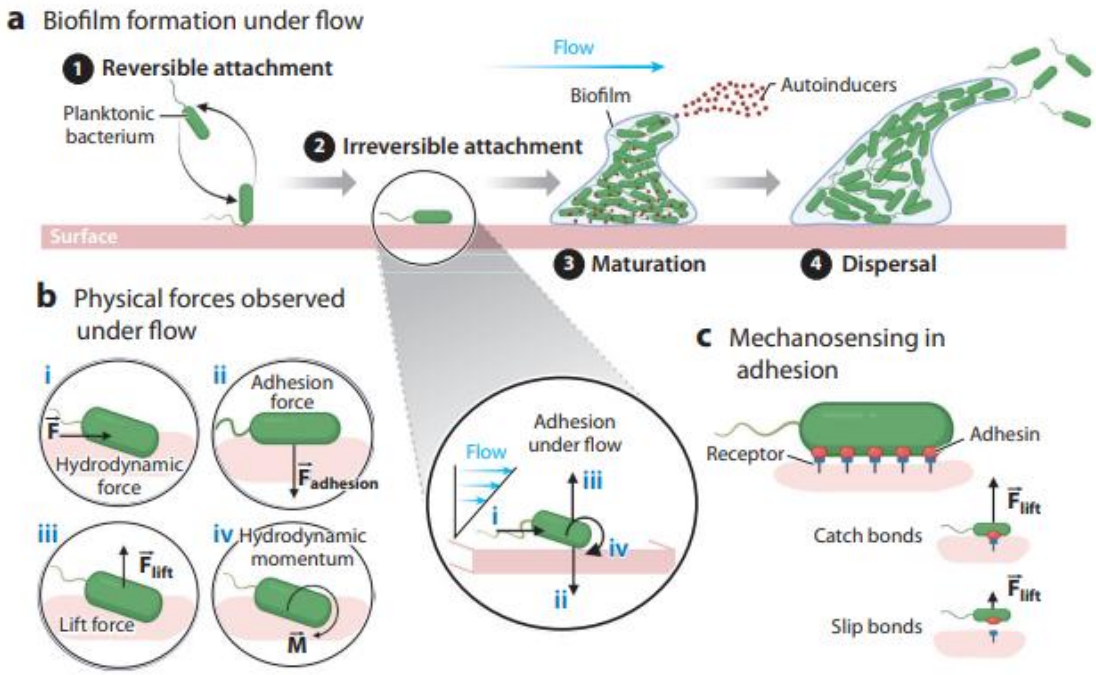

Figure 1.4.2. Describes different stages of biofilm formation under flow (a). (b) shows forces underflow, such as hydrodynamic (i), adhesion (ii), lift (iii) forces, and hydrodynamic momentum (iv). (c) describes mechanosensing in adhesion, when adhesins help bacteria form an attachment to the surface (Yuan et al., 2023).

Therefore, for a precise study of biofilms *in vitro*, flow has to be present to mimic the natural environment as closely as possible. A few new technologies are evolving that enable precise environmental control, one of them being microfluidics. Microfluidics is a technology in which liquids are controlled at a micrometric scale. As mentioned, dynamic methods, although used, lack precise flow control and high–throughput properties (Son et al., 2015).

1.4.3. Types of Microfluidic Chips Used in Biofilm Research

Microfluidic devices have been extensively used for biofilm study and they can be categorized according to their design: chips with linear channels, devices mixing channels, devices with multiple floors, porous devices, topographic, and droplet microfluidics (Pérez-Rodríguez et al., 2022). The design of the channels plays a key role in biofilm formation, adhesion, and growth under a controlled environment. The different geometries of the channel can also impact the biofilm formation. Therefore, as the microfluidic assay is quite versatile, it is really important while designing a microfluidic system to pay attention to the structure of channels and their placement to use it for advancing the research. For example, Cheah & Bae, in 2023, created a multichannel microfluidic platform to study microbial interactions in dual–species biofilms. Their created microchip consisted of several parallel channels enabling real–time monitoring of biofilms' formation under different or identical conditions, and it was stated that microfluidics is a promising tool for biofilm study.

Microfluidic chips can also be integrated with electrochemical biosensors, advancing the study of biofilms in real–time while at the same time providing a controlled environment. These microchips allow a more precise analysis of biofilm dynamics and antimicrobial agents' effects (Fernández–la–Villa et al., 2019).

1.5. Microfluidic chip Fabrication

1.5.1. Materials

Various materials could be used to produce a microfluidic chip, each having their benefits or disadvantages for the experiment. However, the choice of material is considered one of the most crucial steps in its development, and there are several factors to consider when choosing a material. Ideally, it should be transparent for better analysis, it should be chemically compatible with reagents used in the experiment, biocompatible itself, and should be stable and durable (Pan et al., 2018; Shakeri et al., 2019; Sticker et al., 2020). Most commonly used materials include silicon, different polymers such as polydimethylsiloxane (PDMS) or polymethylmethacrylate (PMMA), glass, cyclo–olefin polymers and copolymers (COPs/COCs), and quartz (Focaroli et al., 2014). Silicon has several advantages as a material for microfluidics, as it is chemically compatible, thermostable, has semiconducting properties, freedom in design, and its surface can be modified (Nielsen et al., 2020). Although silicon is one of the most commonly used materials, it is challenging to perform optical analysis of the microchip as its opacity is limited (Mitchell et al., 2024). Glass is another material of choice for microfluidics fabrication. It possesses several advantages, for example, it has greater optical transparency than silicon. Apart from that, it is thermostable, chemically inert, and biocompatible (Hwang et al., 2019). Glass is also considered an environmentally friendly material as microchips produced with it because its chemical stability can be cleaned after an experiment by disinfecting, washing, or even heating up and reused, thus cutting the costs of the experimentation (Ofner et al., 2017). However, working with glass can be time–consuming and expensive to create microchips with it (Campbell et al., 2021). Polymers are a common choice for microfluidic fabrication. PDMS is the most popular because it is cheap, biocompatible, easy to work with, and has high optical transparency and elasticity (Wong & Ho, 2009). Although PDMS is known for its high porosity, and when used in microfluidics, molecules can be absorbed by it, making it unusable with organic solutions (Adamiak et al., 2016). Apart from that, it was observed that microfluidic devices in which PDMS is used tend to change shape under flow, which can lead to inconsistent results (Inglis, 2010). Also, PDMS exhibits a high degree of gas permeability, depending on the specific material chemical formulation. However, it can lead to solvent evaporation within the microfluidic channels, in the end changing their concentrations and affecting the experimental results (Vivas et al., 2010). PMMA offers almost the same qualities as PDMS but does not absorb any molecules (Campbell et al., 2021). Thermoplastics such as COPs/COCs are also a choice when producing a microfluidic chip.

One of the outstanding features is that they can be used with acids, bases, or polar solvents (Bruijns et al., 2019).

1.5.2. The microfluidic chip mold fabrication and 3D printing

The fabrication of a microfluidic chip starts by creating a master mold. The design is a crucial step as it decides what next steps will follow and, in the end, the quality of the experiment. Three–dimensional (3D) printing is an emerging technique that is gaining more attention in microfluidic chip fabrication due to its advantages. 3D printing is a technique when created computer–aided design (CAD) model is printed using various materials to create a 3D structure. This technique allows the creation of various microfluidic chip designs and is an ideal solution to create complicated structures with high fidelity (Lai et al., 2019). Stereolithography is one of the 3D printing techniques used for 3D object production. It uses a laser that, when focused, can solidify the photo–sensitive resin, thus creating a precise structure according to the created 3D model. It is considered one of the cheapest and the most benefits possessing 3D printing techniques, such as high surface resolution and high fidelity from micrometers to millimeters, thus commonly used while fabricating master molds for microfluidic chips (Kotz et al., 2020). Fused deposition modelling is another technique used for mold printing. During the process, thermoplastic material is melted and extruded through a nozzle, which solidifies as it cools off. This method is affordable, fast, and simple, although it could lack precision. The microchannels need extra precision, thus this method could be unsuitable for producing channels at the micrometer level (Pranzo et al., 2018). Therefore, 3D printing stands as a promising technology for master mold fabrication with extra precision, short printing time, and accuracy, minimizing the human error factor. After a mold is printed, a negative replica of the master mold is created using various materials such as the previously mentioned PDMS.

1.5.3. PDMS molding

Printing of master mold and creating a PDMS structure can offer several advantages, one of them extending the use of the master mold, thus making it more convenient for mass production. This approach is known as double casting and is based on a 3D printed mold providing the base for a material of choice, such as PDMS, to be cast and after it possesses the desired features. This approach is quite simple consisting of several steps, described in **Figure 1.5.3**. First, master mold creation, followed by PDMS casting and curing, later separating the PDMS from the mold (Richmond & Tompkins, 2021).

In the literature, this approach is extensively used. Colin et al. 2021 used a consumer–grade stereolithography LCD 3D printer to produce a master mold. After Sylgaard 184 prepolymer was mixed with curing agent. To avoid bubble formation, the PDMS with a mold was subjected to the vacuum. It was noticed that this approach to microchip creation is most trustworthy compared to the

new arising methods, for example, directly printing the microfluidic chip (Wang et al., 2017; Colin et al., 2021).

Figure 1.5.3. Double casting method steps for PDMS molding. Image prepared using biorender.com

1.5.4. Off–stoichiometry thiol–ene

Off–stoichiometry thiol–ene (OSTE) has recently emerged as a new polymer alternative to PDMS for microfluidics fabrication. Although PDMS is considered the most widely used material for microfluidics, it is unsuitable for microchannel fabrication as it has high elasticity and can deform under pressure or high flow rates, ruining the experiment (Hardy et al., 2009). In comparison, OSTE has good mechanical resilience, a high adhesion rate to glass, metals, silicon, or even polymers, and good optical properties. OSTE is a transparent photocurable material formed from thiol and ene monomers with an off–stoichiometry mix ratio. This material is versatile and used in various microfabrication methods such as micromachining, photolithography, casting, injection molding, and fabricating microfluidic chips. One of the best advantages of OSTE is its direct and rapid surface modification and fast curing time, approximately 30 seconds (Carlborg et al., 2011).

1.6. Biofilm analysis methods using a microfluidic chip

One of the most important aspects of any experiment is the method of analysis chosen. The scientific community uses several methods to study biofilms in microfluidics. The analysis method is chosen according to microfluidic chip properties, such as materials used in fabrication or data needed to acquire from the experiment. For example, light microscopy could be used to evaluate bacterial adhesion if biofilms are formed on PDMS (Straub et al., 2020). Another one of the classical methods to evaluate the biofilm is colony–forming units (CFUs). CFUs is a standard unit of measurement of biofilm growth applied in microbiology and molecular methods. CFUs number is determined after cell colonies are formed using a specific growth medium in specific conditions. The limitation of CFUs is that it allows the counting only of microorganisms that can be cultivated and is time–consuming (Li et al., 2014). Light microscopy and CFUs are affordable and widely used methods for analysis. However, more profound imaging could provide information about biofilm growth,

adhesion, and their response to the environmental changes at the cell level over time, such methods include– fluorescence and electron microscopy or optical coherence tomography (OCT) (Rodrigues et al., 2023). Confocal laser scanning microscopy (CLSM) is a technique based on selectively excited fluorescence signals in a sample, which generates images with localized laser excitation at specific wavelengths point by point. This method enables biofilm visualization in a 3D form, allowing the acquisition of information on biofilm viability, architecture, surface coverage, and thickness (Mountcastle et al., 2021). CLSM is often used as a non–invasive or an *in situ* analysis method, as the fluorescence signals come from staining probes or bacteria that are fluorescent– tagged, allowing to obtain information on biofilm distribution in a non–destructive manner, even at the single–cell level (Straub et al., 2020). CLSM allows biofilm growth in real–time monitoring (Tran et al., 2022) and can be implemented together with transmitted detector (TD) function, allowing visualisation of the microchip channel middle–depth plane, thus more accurately analysing the biofilm coverage of the channel (**Figure 1.6.**) (Wei & Yang, 2023). However, CLSM has a few drawbacks– it cannot be used for thick biofilm analysis (Yuan et al., 2020).

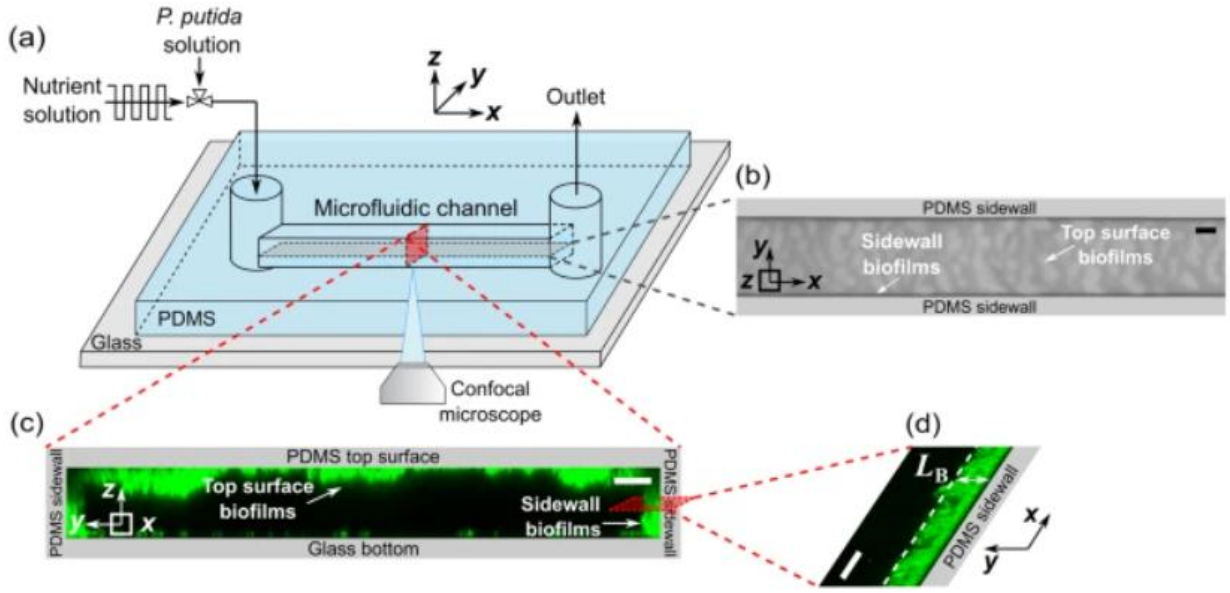

Figure 1.6. Visualization of experimental setup for analysing biofilm development in the microfluidic chips channel (a). The *x*, *y*, and *z* axes, respectively, represent the flow, lateral, and vertical directions. (b) shows a CLSM image, showing a horizontal cross–section of the microfluidic chip channel, captured using TD. (c) 3D reconstruction of biofilm dyed with fluorescent dyes in the vertical y–z plane, as shown in a). (d) magnified CLSM image showing biofilm formation against the channel walls in the x–y plane. LB indicated average biofilm thickness. The scale bar is 25 μm. The visualization was adapted from Wei & Yang, 2023.

However, CLSM has a few drawbacks– it cannot be used for thick biofilm analysis (Yuan et al., 2020). OCT is seen as an alternative method for CLSM as it is also non–invasive and allows real–time monitoring of biomass and thickness of biofilm. OCT offers quite a wide range of depth

analysis– from several millimeters up to 20 mm. One disadvantage is that it's impossible to analyse early biofilm formation or bacteria at the single–cell level (Xi et al., 2006). Electron microscopy, especially scanning electron microscopy, offers a detailed analysis of biofilms. Bacteria structures such as pili, surface or cell–to–cell, or cell to the surface can be analyzed. Although this method offers advantages that CLSM and OCT lack, it is an invasive and time–consuming technique (Arunachalam & Davoodbasha, 2021). Therefore, choosing the analysis method that would fit the experiment platform and fulfill all the data requirements needed to acquire is important.

2. METHODOLOGY

2.1. Materials

Materials used in this study:

1. COC Topas microscopy slide format (75.5 mm × 25.5 mm), Microfluidic ChipShop, Jena, Germany.
2. Sylgard 184 silicone elastomer kit (Dow Corning, USA).
3. Zortrax white resin (Olsztyn, Poland).
4. OSTE resin (Ostemer 322) (Mercene Labs, Sweden).
5. PTFE tubing with a 1/32" inner diameter (Darwin Microfluidics).
6. Brain Heart Infusion broth (Biolab, Hungary).
7. Ciprofloxacin (Thermo Fisher Scientific, USA).
8. Tetracycline (Thermo Fisher Scientific, USA).
9. MycoLight bacterial viability assay kit (AAT Bioquest, USA).
10. Isopropyl alcohol (Eurochemicals, Lithuania).
11. Acetone (Sigma–Aldrich, Germany).
12. Disodium hydrogen phosphate anhydrous (Applichem, Germany).
13. Natriumchlorid (CarlRoth, Germany).
14. Potassium chloride, ACS reagent, 99.0–100.5% (Sigma–Aldrich, Germany).
15. Potassium dihydrogen phosphate (Sigma–Aldrich, Germany).
16. Trypsin from porcine pancreas (Sigma–Aldrich, Germany).
17. Ethylenediaminetetraacetic acid disodium salt dihydrate (VWR Chemicals, Belgium).
18. Pseudomas Isolation agar (Milipore, Germany).
19. CHROMagar Staph aureus (CHROMagar, France).
20. CHROMagar e.O157 (CHROMagar, France).

2.2. Microfluidic chip fabrication

This section presents the design and fabrication process of microfluidic chip. Considering the complexity of the five–channel setup, the chip went through a series of processes to ensure high quality performance and reliability. Each part of the fabrication process highlights various methodologies, such as CAD creation, 3D printing, material preparation, and the assembly of the chip, to achieve the most precise results after implementing this platform for biofilm study. This methodology describes all necessary steps to create a microfluidic system.

2.2.1. Master mold printing

Master mold printing starts from the creation of the design using Autodesk Fusion 360 CAD modelling software. For printing Zortrax Inkspire 3D printer was used together with Zortrax white resin. After the design creation, the mold model is exported in a STL or OBJ file format, which is required for it to be 3D printed (**Figure 2.2.1.**). After uploading the 3D printable file into the printer's software and before starting the printing process, it allows user to choose the printing parameters such as slicing layer thickness or exposure to UV light time. This is a relatively quick negative master mold production process as it can produce several molds with high accuracy, thus minimizing the mistake rates. After the printing process, the master mold is cleaned with isopropyl alcohol (IPA) to remove any uncured resin and is additionally cured with UV light to strengthen its mechanical properties to acquire the final product.

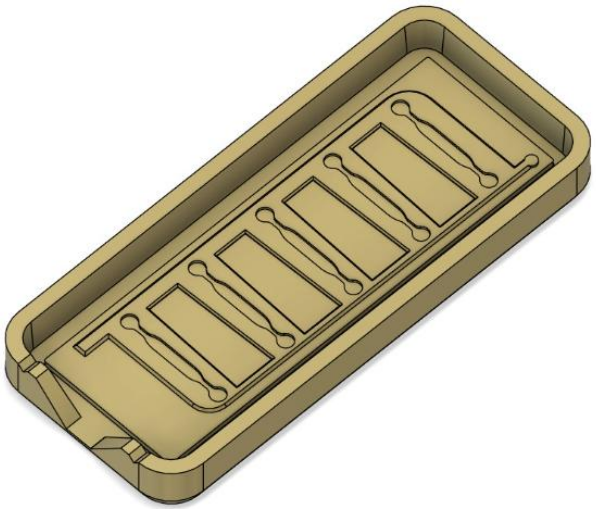

Figure 2.2.1. 3D model of the master mold for PDMS casting.

2.2.2. Casting of PDMS

After fabricating the positive master mold, PDMS was casted. PDMS was produced using SYLGARD silicone elastomer and mixing base and curing agent at a 10:1 weight ratio. After mixing, any bubbles that formed were removed using a vacuum chamber. Then, the silicone elastomer was poured into the printed master mold to acquire the desired pattern. The constructed master mold, together with the silicone elastomer, was cured for 24 hours at 60 °C (**Figure 2.2.2.**). After curing, the negative PDMS mold was hardened, removed, and washed with IPA to eliminate any remaining

residue.

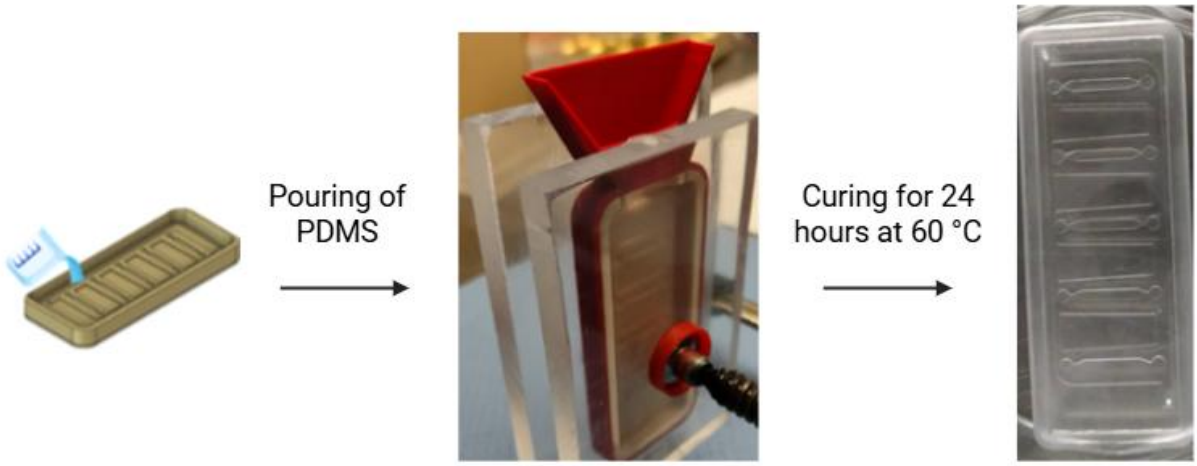

Figure 2.2.2. Process of PDMS casting, the last photo shows the final PDMS mold.

2.2.3. COC preparation

The designed microfluidic chip is assembled using two COC substrates: a Microscopy slide format (bottom COC) and a microscopy slide Luer platform with ten fluidic interfaces (top COC). Before using both COCs for the microfluidic chip, they need to undergo several preparation steps. Firstly, to enable fluid to pass through the top COC into the microchannels holes are drilled precisely in the connection centers. After the COCs are cleaned with acetone and rinsed with IPA, they are ultrasonically cleaned for 10 minutes. Ultrasonic cleaning is a method that uses an ultrasound to thoroughly clean difficult–to–access places by agitating a fluid flow, achieving the best cleaning level. Then, oxygen plasma treatment follows. This type of treatment is described as a surface modification technique that interacts with the surface, removes any organic contamination, and enhances the adhesion, which is critical to the microfluidic chip assembly. The oxygen plasma (Zepto B, Diener Electronic, Germany) treatment is performed using 50% power, 0.35 mbar pressure for 90 seconds.

2.2.4. OSTE injection

Another important step in the microfluidic chip fabrication process is OSTE preparation and injection. The entire process is demonstrated in **Figure 2.2.4.** and **Figure 2.2.5**. OSTE resin was prepared by mixing two components: Part A (1.09): Part B (1.0), w/w. The device including the produced negative PDMS mold and bottom COC is assembled using springs to ensure even pressure on the COC. Using a syringe and tubing, OSTE was injected into the assembled device, which was placed at a 45–degree angle. Following the injection, the UV light is then used to seal the last microfluidic chamber to facilitate the passage of any bubbles that may occur. After injection, the initial curing is performed with 365 nm UV light at an intensity of ~2.04 mW/cm² for 18.5 seconds.

Then the whole device is disassembled, and the top COC with the sticky OSTE pattern is carefully removed from the negative PDMS mold.

Figure 2.2.4 OSTE injection procedure in the lab.

2.2.5. Assembly of the microfluidic chip

To ensure a steady flow through the channels in the microfluidic chip, the top COC with a sticky OSTE pattern was carefully aligned with the top COC so that the previously drilled holes match the pattern. The assembled chip is then pressed using metal plates and cured at 60 °C for 4 hours to fully polymerize OSTE, enhance bonding, and ensure efficient sealing of the microfluidic chip.

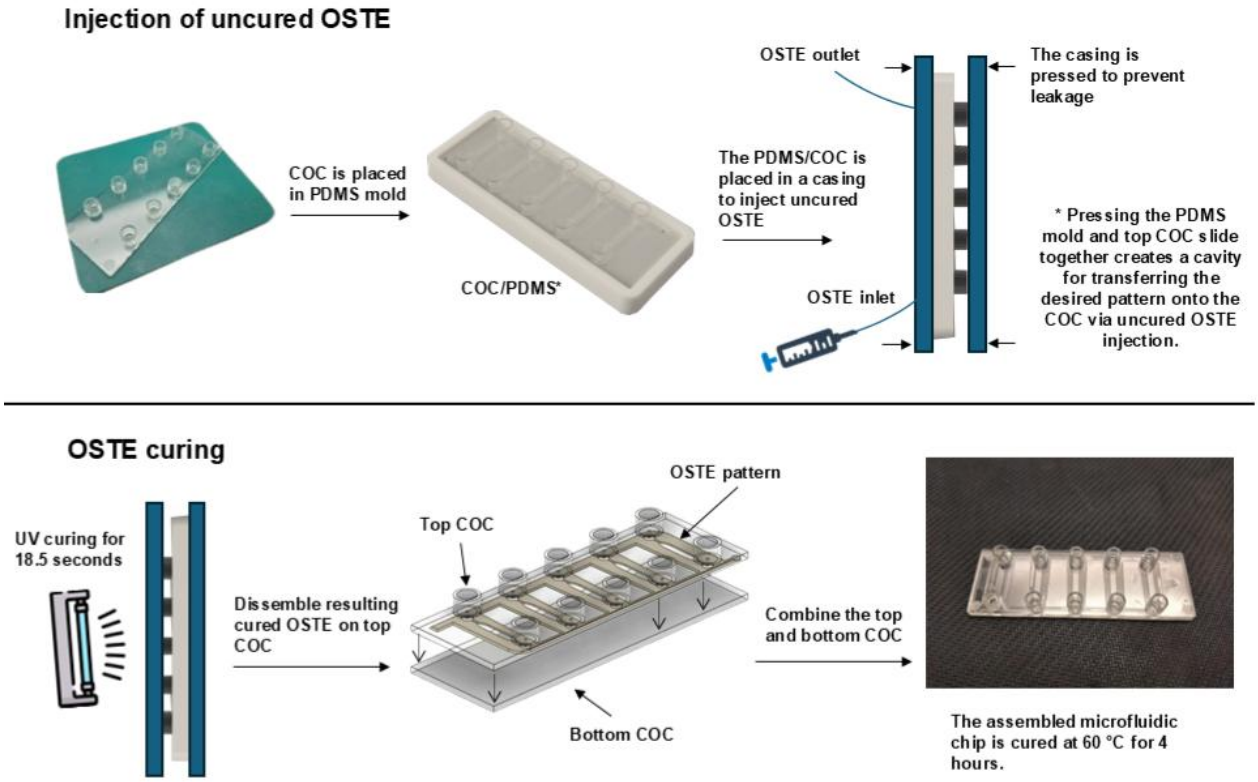

Figure 2.2.5. The process of OSTE injection, curing and assembly of the microfluidic chip.

2.2.6. Microfluidic platform sheer stress analysis

Wall shear stress (WSS) distributions were analyzed to assess shear forces in the channels and chambers. The findings emphasized areas of consistent shear alongside regions with heightened stress, notably at channel junctions and near chamber inlets. Average and peak WSS values were documented to evaluate the shear environment affecting the biofilm. These simulations offered insights into the mechanical conditions within the microfluidic chip, confirming that the design was appropriate for investigating biofilm growth under regulated shear stress conditions.

2.3. Biofilm growth in the microfluidic chip

For microbial biofilm growth, the developed microfluidic chip described earlier was used. Three different strains of bacteria: *Pseudomonas aeruginosa* (PAO1), *Staphylococcus aureus* (ATCC 25923), and *Escherichia coli* (K12, DMS498) were used in this study. Firstly, the bacteria were cultivated aerobically in the incubator at 37 °C and 150 rpm in BHI until they reached the mid–logarithmic phase. Cultures were centrifuged for 5 minutes at 5000 rpm and washed three times with PBS. Using a spectrophotometer set to a wavelength of 620 nm, a final concentration of 1×10^7 cells mL^{-1} was prepared. To allow initial cell adhesion to the surface, the microfluidic chip channels were then filled with the cell suspension using a micropipette and incubated under static conditions for 1.5

hours at 37 °C temperature. To initiate the polymicrobial biofilm formation and adhesion phase, *E. coli* or *P. aeruginosa* was introduced and incubated for 1.5 hours in the channels. Then, the channels were washed three times with PBS, and *S. aureus* was introduced and incubated under the same conditions for 30 minutes. Following the initial bacterial adhesion, the microfluidic chip was connected through tubing to a syringe containing fresh BHI growth media using the pumping system (**Figure 2.3.**). The BHI was flowed through the channels at a rate of 5 µL/min for the various durations specified in the results section. Subsequently, PBS was perfused through the channels at a flow rate of 5 µL/min for 30 minutes to prepare the chip for further experimentation and to remove any waste formed during growth.

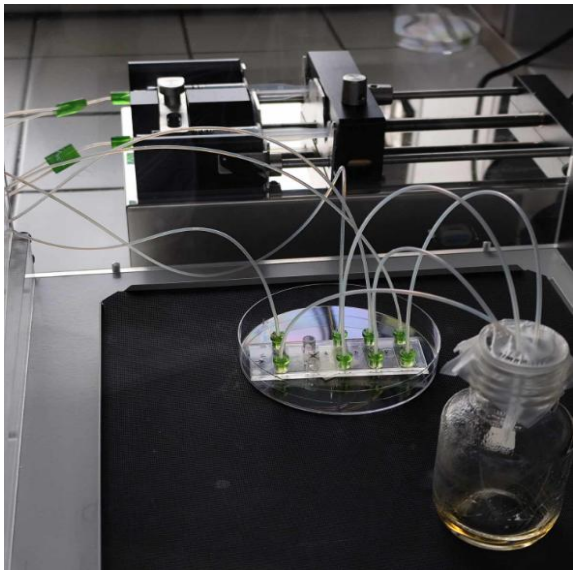

Figure 2.3. Microfluidic system set up using the pumping system.

In this study, monomicrobial and polymicrobial biofilms were grown, thus, two slightly different methods were used to ensure that the polymicrobial biofilm formed in the channels. The first method involved bacteria dyeing using MycoLight bacterial viability assay kit and analysis using a confocal microscope. In contrast, the second method involved the chemical removal of the biofilm from the channels. Trypsin, an enzyme commonly used to detach adhered cells from the surface, was introduced into the channels to detach the formed biofilm from the channel's surface. Trypsin treatment was carried out for 30 minutes, and the volume was collected with a micropipette into a separate tube. New syringes with 5 mL of PBS were prepared and replaced in the flow system, and the channels were washed to fully remove any cells after trypsin treatment. The gathered bacterial cell suspensions were centrifuged and diluted. The *E. coli* bacteria were diluted 10 times, while *S. aureus* was diluted 20 times. The cell suspension was then seeded on agar plates and left to grow for 16 hours in a static manner in the incubator. After growth, the formed colonies were counted.

2.4. Biofilm antimicrobial treatment

Biofilms that had been grown for 48 hours were then exposed to ciprofloxacin for 16 hours at a concentration of 5 μg/mL. Additionally, *S. aureus* bacteria were grown in a microfluidic chip for 48 hours and exposed to different concentrations of tetracycline (32 μg/mL, 64 μg/mL, 128 μg/mL) for 16 hours. To ensure the biofilms maintained constant contact with the antibiotic during treatment, a medium flow rate of 5 μl/min was kept. Following the treatment, the biofilms were rinsed with sterile PBS at a flow rate of 5 μl/min for 30 minutes, allowing for the cleaning of the microchannels and the removal of any loosely attached or residual bacteria.

2.5. Biofilm growth in 24–well plates

For the initial testing of biofilm growth under static conditions, they were grown in 24–well plates and prepared in the same manner as for the microfluidic chip. After preparing the final bacteria suspension, 1.5 mL of the final cell volume was introduced into the wells and incubated under static conditions at 37°C for 1.5 hours to facilitate initial cell adhesion. The wells were then washed three times with PBS, and for growth, 3 – 4 mL of BHI was added to the wells and the plates were left in the incubator for a specific period, depending on experiment requirements, at 37°C with 50 rpm. After incubation, BHI was removed from the wells, and the cells were washed three times with PBS to remove any residual waste. Bacteria visualization was performed using the MycoLight bacterial viability assay kit, and the working solution was prepared as described in the assay manual. To each well 100 μL of dye solution was added and left to stain for 25 minutes in the dark at room temperature. The wells were washed three times with PBS to remove excess stain, and samples were prepared for visualization with a confocal microscope.

2.6. Colony forming unit biofilm growth and analysis

The colony–forming unit (CFU) assay is one of the most popular methods in microbiology labs that allows the detection of the number of viable bacteria in the sample. The bacteria were prepared in the same manner as during the 24–well plate assay and left to grow with BHI for a specified time. However, for polymicrobial biofilm, the incubation times differed:

1. For polymicrobial biofilms, 1.5 mL of *P. aeruginosa* and *E. coli* cell suspension was first introduced to the wells and incubated for 1.5 hours.
2. The wells were then washed three times with PBS, and 1.5 mL of *S. aureus* suspension was introduced. Later on, the suspension was incubated at the same conditions for 30 minutes.

After growth, bacteria were washed with PBS, scraped, and diluted. The dilution factor differed for each bacterial strain: for *P. aeruginosa* and *E. coli*, 10^{-3}, and for *S. aureus*, 10^{-6}. After the final

dilution, 20 µL of bacteria were seeded in agar plates and incubated for 16 hours. Afterward, formed colonies were counted to assess the number of viable cells.

2.7. Analysis using confocal scanning microscopy

Using a Nikon Eclipse Ti2 confocal laser scanning microscope with a 20× objective lens, stained biofilms were visualized. Fluorescence detection occurred at an excitation wavelength of 488 nm, with emission filters set to 510–530 nm for MycoLight™ Green indicated live cells and 600–660 nm for propidium iodide indicated dead cells. Biofilm images were captured using an Andor Zyla sCMOS camera linked to the DSD2 differential spinning disc system, ensuring high–resolution and precise fluorescence detection. For 3D visual reconstruction of the biofilm structure, Z–stack images were collected at 1 µm intervals. Finally, data was collected using Nikon Elements software, and image analysis was performed using ImageJ (Fiji) software.

3. RESULTS

3.1. Microfluidic chip fabrication and quality control

The main objective of this study was to create a reliable platform for investigating microbial biofilms under controlled conditions. Thus, we successfully developed a microfluidic chip consisting of five separate growth chambers. The separate chambers allow testing different experimental conditions in one run while precisely manipulating fluid flow and shear stress, which are crucial factors in biofilm formation under dynamic conditions. The size of the microfluidic chip was produced according to the standard microscope slide dimensions (75 mm × 25 mm), making it an ideal candidate for use with various imaging tools for biofilm analysis.

The chip's fabrication process, as described in the methodology, began with 3D printing a positive master mold, which was then used to create a negative PDMS mold. OSTE resin was injected into the top COC and PDMS mold casing to ensure durable and precise microchannels. The final step involved assembling the microfluidic chip by bonding COC to the patterned mold using plasma treatment. This bonding method minimized the possibility of leakage while creating an environment free of contamination, which was confirmed by the lack of leakage during perfusion through the channels. Apart from leakage, validating microfluidic chip functionality is an important factor to consider after the fabrication process. In this study, the chip's functionality was tested by injecting a fluorescent dye into the channels and observing the fluid flow with confocal microscopy. The fluorescence intensity profile analysis showed that the dye's flow was even in all growth chambers without the formation of dead zones or blocked channels. These results prove that the created microfluidic design enabled consistent and stable fluid flow under the specific experimental conditions.

Another important factor to consider when fabricating microfluidic chips is the scaling up of the production, which is crucial for future biofilm studies. The fabrication process must be repeatable to ensure the same chip quality during each fabrication, thus, it is important to assess channel variation across several produced chips and in each chip separately. The measurement of microfluidic channels showed that the variation of dimensions was less than ±3%, confirming the possible production scalability while maintaining quality.

3.2. Improvements in microfluidic chip fabrication and system setup

During the microfluidic chip fabrication process, multiple chips were produced to achieve the optimal design and functionality. Since the entire process can be time–consuming, several attempts were made to reduce the fabrication time through improvements in methodology. Considering that the produced microfluidic chip is used for biofilm growth and analysis, various challenges emerged that needed to be addressed, not only in the fabrication process but also in setting up the entire

microfluidic system. Recognizing all the challenges and improvements made during the development process, key changes and their outcomes are outlined in the table below (**Table 1**).

Table 1. Changes made in the chip and comparison

Primary methodology	**New methodology**	**Result**
Master mold design	New master mold design	The updated master mold pattern resolved the issues that occurred during OSTE injection, such as bubble exit from the assembled COC and PDMS casing. The new design features rounded edges and larger chambers, which are crucial for biofilm formation and minimizing the risk of leakage.
OSTE injection when COC and PDMS casing positioned horizontally	OSTE injection with COC and PDMS casing positioned at a 45–degree angle	The COC and PDMS casing placement at 45 degrees allows the bubbles to pass during OSTE injection, thus minimizing the risk of entrapped bubbles and possibility of failed fabrication of microfluidic chip.
Entrapped bubbles in the OSTE pattern during injection	The UV light is used to seal the last microfluidic chamber to encourage the passage of bubbles.	To further prevent the entrapped bubbles in the OSTE pattern, the last chamber was sealed using UV light for 5 seconds. This enabled a more fluent flow of the OSTE through the COC and PDMS casing and helped to remove any stubborn bubbles, ensuring an even pattern after curing.
The OSTE pattern casted on bottom COC	The OSTE pattern casted on top COC	Casting the pattern on the bottom COC posed multiple challenges, including the precise alignment needed with the top COC ports, which led to several failed microfluidic chips. By moving the pattern casting to the top COC, this issue was resolved, simplifying the final assembly of the chip and relatively reducing the production time.

Primary methodology	New methodology	Result
High leakage rates occurring in the microfluidic chip during experiments.	Mitigating the risk of leakage before establishing the microfluidic system	Before each experiment, the chip was tested for leakage to minimize the number of failed experiments. Distilled water was slowly introduced into the channels to ensure each channel was filled without water flowing into other channels or through the entire chip.
The pump contained syringes with multiple tubes extending from a single syringe.	The syringe in the pump has only a single tube extending from it.	Using multiple tubes connected to one syringe allowed for various experiments to be performed with fewer pumping systems. However, this setup led to inconsistent flows of BHI or PBS, which resulted in unreliable results or experimental failures. In contrast, utilizing a single syringe with one tube to deliver media into a single chamber produced reliable results and consistent flow during the experiment, significantly decreasing the number of failures.

This enhancement process emphasizes a reliable improvement approach in producing microfluidic chips for biofilm studies. The advancements listed in **Table 1** not only pave the way for reliable chip production in the future but also guarantee that the high quality of chips remains consistent.

3.3. Distribution of Wall Shear Stress in the Microfluidic Channel

Wall shear stress (WSS) is a force that affects fluid flow in the channels. It is considered a critical parameter while creating microfluidic chips for biofilm study, because it affects how biofilms forms. In this study, WSS was tested using ANSYS Fluent, a computational fluid dynamics software that uses mathematical modelling to simulate fluid flow and other physical aspects in complex geometries, such as microfluidic chips for testing laminar flow or WSS. The software provided a detailed shear force distribution throughout the channel walls and visualised where the force was the highest and the lowest (**Figure 3.3.**). It was observed that the WSS varied in the channel, and the highest stress was near the outlet and inlet regions, marked red, decreasing gradually towards the center of the channel.

In the narrowest part of the chip, due to the geometry of the channel, the flow velocity increased, and the maximum WSS value was calculated, reaching 5.44×10^{-3} Pa. The lowest WSS of 0 Pa was observed in the channel regions where the flow was stagnant and near channel walls, where fluid motion is low. The most uniform shear stress distribution was in the center parts of the chip, where values ranged between 1.81×10^{-3} Pa and 3.17×10^{-3} Pa, which reflected the steady flow conditions set in the simulation. These results show that a consistent flow and shear stress are produced in the channel, confirming that the design allows gathering reliable and repeatable results under controlled conditions.

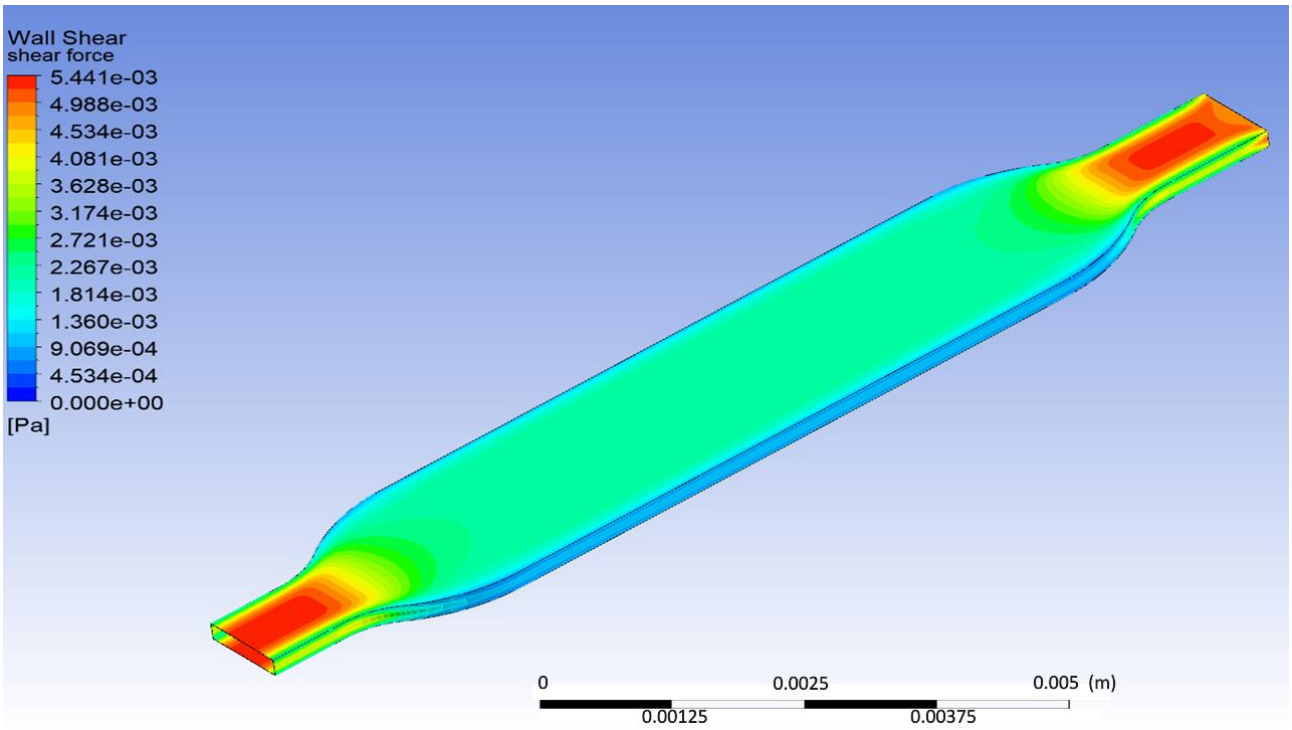

Figure 3.3. Wall shear stress distribution in the microfluidic channel assessed using ANSYS Fluent. The color distribution represents WSS values in Pascals, with the highest stresses marked red and observed near the inlet and outlet, and the lowest stresses marked blue.

3.4. Monomicrobial biofilm growth under static and dynamic conditions

As microfluidic chips are considered a relatively new method for studying biofilms, to confirm the reliability of our produced chips in a laboratory setting, bacteria were also grown using a routinely used method in microbiology–cell growth in well plates. Two bacteria species biofilm growth: *P. aeruginosa* and *S. aureus* was monitored at different time points: 3, 24 and 48 hours after initial cell adhesion for dynamic (microfluidic chip) and static (24–well plate) growth methods, after initial cell adhesion phase. Each time point represents a stage in biofilm formation, 3 hours–initial bacteria adhesion, 24 hours– maturation phase, and 48 hours– biofilm maturation phase 2. The confocal microscopy analysis photos are presented in **Figure 3.4**.

After 3 hours of growth under dynamic conditions, both bacteria species formed isolated cell clusters, indicated by higher fluorescence across the channel surface, and in general, the cell adhesion was scarce. In comparison, under static conditions, both bacteria's adhesion, according to the fluorescence intensity, was denser, especially for *P. aeruginosa*, confirming that the initial adhesion is more rapid and higher in density when shear force is not present.

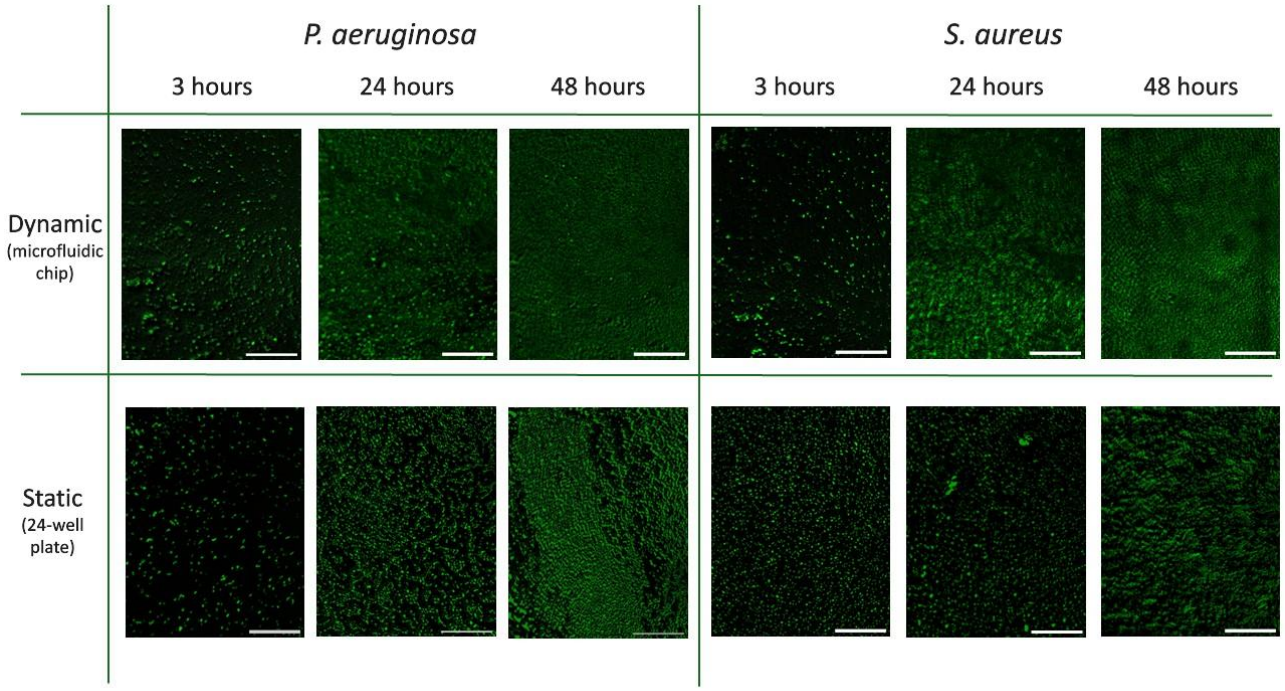

Figure 3.4. Confocal microscopy analysis of *P. aeruginosa* and *S. aureus* biofilm formation under dynamic (microfluidic chip) and static (24–well plate) conditions at 3, 24, and 48 hours.

At the 24–hour time point, the divergence in biofilm formation under different conditions started to show. Bacteria grown in dynamic conditions showed that under the influence of shear force, uniform biofilm layers with even coverage are formed, as seen in the *P. aeruginosa* sample. As *P. aeruginosa* growth is known to be challenging, the biomass was less increased compared with *S. aureus* under dynamic conditions. *S. aureus* biofilm maintained structural integrity while the biomass was substantially increased compared to the 3– hour sample. *P. aeruginosa* bacteria grown in static conditions formed dense cell clusters, while *S. aureus* formed more uneven layers across the surface.

After 48 hours, the difference between bacteria grown in static and dynamic conditions became even more visible. Under dynamic conditions, both bacteria continued to form thin and evenly covering the surface biofilms. While under static conditions, *S. aureus* formed thicker and more uneven mats, and *P. aeruginosa* formed heterogeneous and thick cell clusters. Overall, the results confirm the importance of shear force in biofilm formation, as it restricts the biomass growth vertically, hence, forming thin, but more homogenous biofilms. As for static conditions, bacteria tend to form irregular biofilms and grow excessively, as there are no forces restricting the growth, resulting in rapid, irregular biofilm accumulation.

3.5. Antibacterial treatment of microbial biofilms with the microfluidic system

To evaluate the microfluidic chip`s potential to be used as a dependable platform for screening antimicrobial treatments on biofilms, the antibiotics ciprofloxacin and tetracycline were used. For ciproflocaxin treatment efficacy evaluation, *P. aeruginosa* and *S. aureus* bacteria were grown for 48 hours under dynamic conditions and for tetracycline–only S. aureus were treated. Using fluorescence dyes, bacterias` biofilms were visually analysed to distinguish between the quantity of live and dead cells. Biofilm thickness was also measured, and any structural changes were assessed using 3D confocal microscopy.

The untreated *P. aeruginosa* and *S. aureus* control samples grew dense, homogenous biofilms with a strong green fluorescence signal, indicating a high presence of viable cells (**Figure 3.5.1.**). Ciprofloxacin (5 µg/mL) treatment was applied for 16 hours under dynamic conditions, which resulted in a decreased number of viable cells and disrupted structure, shown by decreased green color and increased red color fluorescence. In the *P. aeruginosa* sample, after treatment, the biofilm`s biomass reduced and became heterogeneous. In contrast, the *S. aureus* sample, after treatment, also became heterogeneous, less dense, with some patches of intact biofilm.

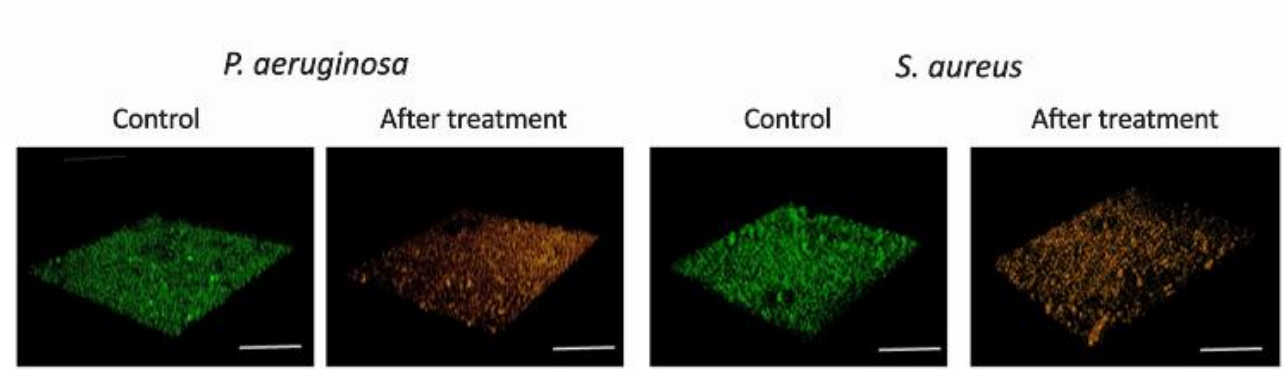

Figure 3.5.1 3D confocal microscopy images of biofilms after 48 hours of growth in a microfluidic system. Control samples with green fluorescence show homogenous and viable biofilms, while samples after treatment show increased red fluorescence with disrupted structures, indicating significant cell death. Scale bars represent 100 µm.

Apart from visual analysis, biofilm thickness was assessed using quantitative analysis to confirm the structural changes observed during visual analysis of confocal images (**Figure 3.5.2.**). For this reason, the biofilm thickness was measured. In untreated samples, *P. aeruginosa* displayed an average of 21 µm thickness, and after treatment, it decreased to 18 µm. A similar decrease was observed in *S. aureus* samples after treatment, the thickness decreasing from 32 µm to 24 µm. These results confirm that the antimicrobial treatment was successful, and the produced microfluidic chip can be used to study the effects of antimicrobial treatments for microbial biofilms under controlled flow conditions.

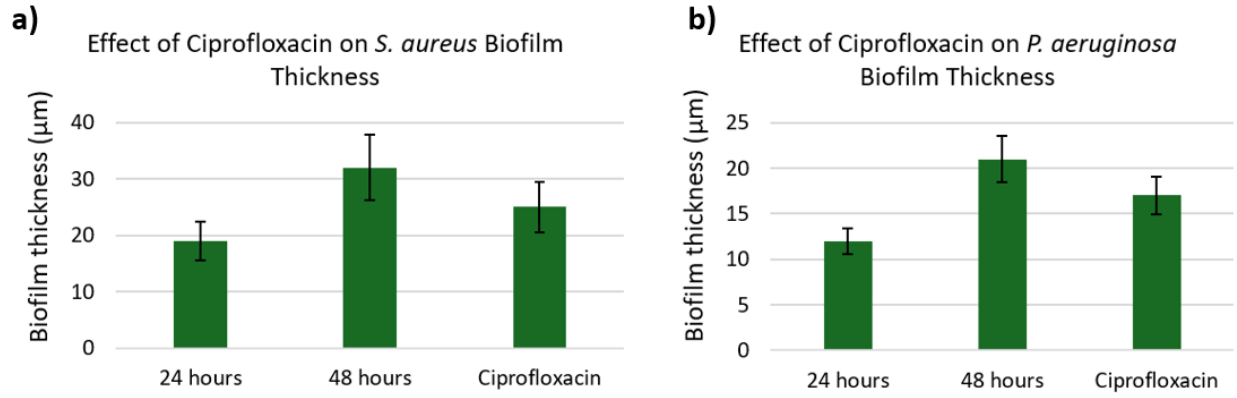

Figure 3.5.2. Quantitative measurements of *S. aureus* (a) and *P. aeruginosa* (b) biofilm thickness at 24 hours, 48 hours, and post–treatment with ciprofloxacin (5 µg/mL) for 16 hours.

To assess the efficacy of different concentrations of antibiotic treatment on biofilms, *S. aureus* was treated with different concentrations of tetracycline (**Figure 3.5.3.**). The untreated, control sample after CLSM analysis showed dense and even biofilm with a strong green fluorescence signal, suggesting that there is a high amount of viable cells. After the lowest antibiotic concentration (32 µg/mL) treatment, the red fluorescence indicating dead cells starts to appear, with disrupted biofilm and the start of biofilm degradation. Increased antibiotic concentration (64 µg/mL) results in a significant increase of red fluorescence signal, emphasising reduced bacterial activity, followed by biofilm degradation. At the highest concentration (128 µg/mL), red fluorescence dominates, with highly dispersed and sparse biofilm, showing significant bacterial death and biofilm eradication. These results show that fabricated microfluidic chip is a reliably platform to study dose dependent antibiotic effects on microbial biofilms.

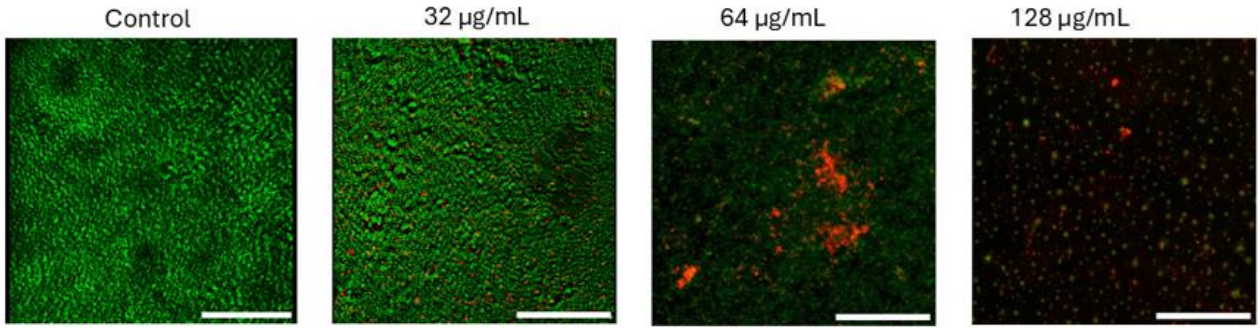

Figure 3.5.3. 3D confocal microscopy images of *S. aureus* biofilms after 48 hours of growth in a microfluidic system after treatment with different concentrations of tetracycline. Control sample (without treatment) shows enhanced green fluorescence displaying viable and dense biofilm, while samples after treatment with varying concentrations of antibiotic show increased red fluorescence, indicating significant cell death with disrupted and almost eradicated biofilm. Scale bars represent 100 µm.

Quantitative analysis was performed to confirm the structural changes observed in CLSM images after tetracycline treatment (**Figure 3.5.4.**). The graph illustrates the effects of different concentrations of tetracycline on *S. aureus* biofilm thickness, grown for 48 hours, after 16 hours of treatment at 5 µg/mL flow rate. In the control sample, where treatment was not applied, biofilm reached approximately 38 µm thickness, displaying robust biofilm formation. With a 32 µg/mL tetracycline concentration, biofilm thickness reduced to 33 µm, showing the initial biofilm response to the antibiotic. Higher concentrations of antibiotics showed a significant decrease in thickness, with 64 µg/mL the average thickness being 16 µm, and for 128 µg/mL, decreasing to less than 6 µm, demonstrating almost complete disruption of the biofilm structure. These quantitative results confirm the observations gathered from CLSM analysis and confirm that the microfluidic chip can be recognized as a reliable platform for dose–dependent antibiotic studies on biofilm reduction and eradication.

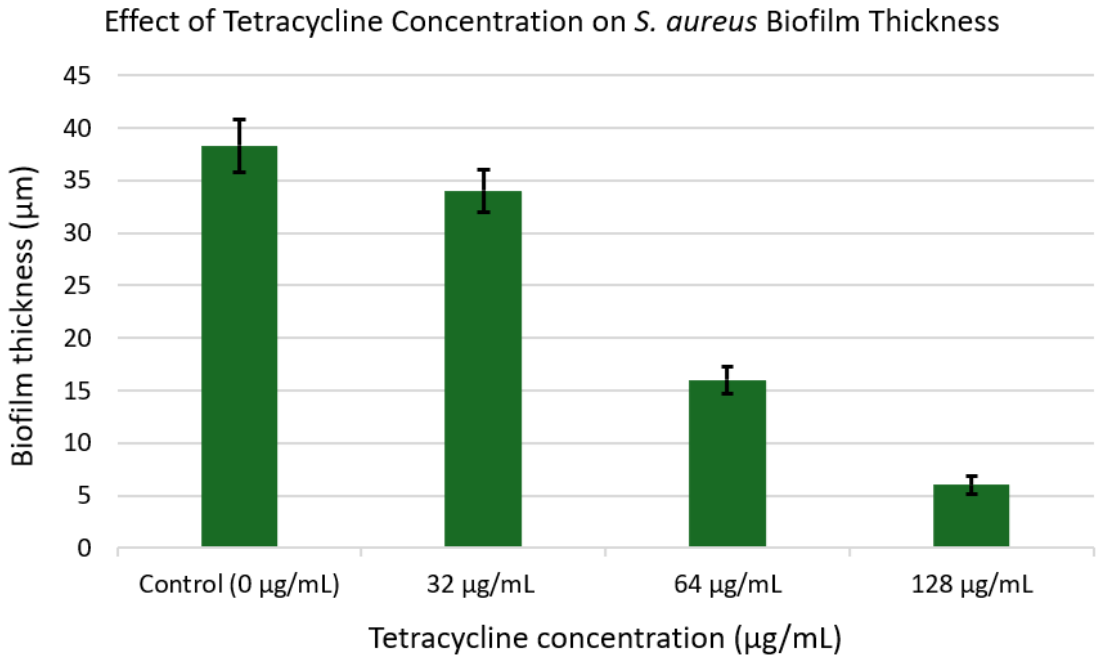

Figure 3.5.4. Quantitative measurements of biofilm thickness grown for 48 hours, after 16 hours of tetracycline treatment for 16 hours, with different concentrations (32, 64, 128 µg/mL).

3.6. Polymicrobial biofilm growth

To further expand the produced microfluidic chip features and capabilities, polymicrobial biofilm (PMBF), including *E. coli* and *S. aureus*, was grown. Firstly, a CFU assay was conducted to compare and test PMBF growth in static conditions; the results of the CFU assay are shown in **Figure 3.6.1**. It was observed that *S. aureus* formed mono–biofilms under static conditions and was present in the PMBF sample, represented by several colonies formed on an agar plate in **Figure 3.6.1.** parts **a)** and **b)**. However, monocultured *E. coli* did not form the biofilm, nor was it present in the PMBF sample, which is represented by the absence of colonies on the agar plate. This could have happened

because of several reasons, for example, compared to *S. aureus*, *E. coli* is known to detach more easily from the surface, thus, if samples were washed harshly, it would enhance the biofilm detachment and eliminate bacteria from the wells.

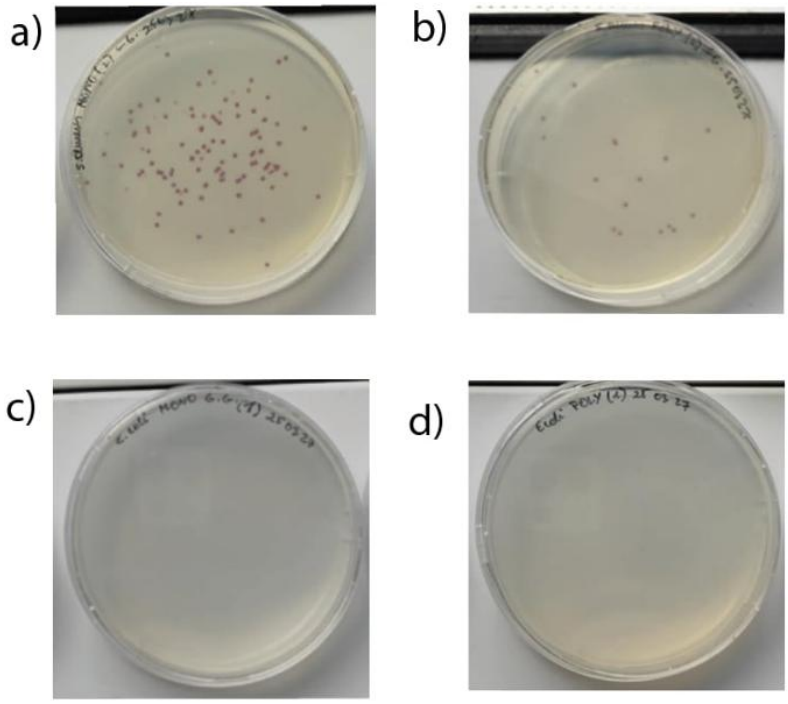

Figure 3.6.1. CFU assay results of *S. aureus* and *E. coli* grown under static conditions for 48 hours. a) Monoculture *S. aureus* biofilm, shows several formed colonies, b) *S. aureus* collected from a polymicrobial biofilm cultured together with *E. coli*, showing dominant growth of *S. aureus*, c) Monoculture *E. coli* biofilm, demonstrating no formed colonies, d) *E. coli* from the polymicrobial biofilm, showing lack of growth.

The experiment was repeated in the developed microfluidic chip to test how bacteria form polymicrobial biofilms under dynamic conditions. Firstly, to ensure that PMBF forms after the growth in the microfluidic chip, bacteria were chemically detached, using trypsin, from the channel surface, diluted, and seeded on selective agar plates. The results are presented in **Figure 3.6.2**. The biggest difference is that *E. coli* bacteria formed a higher count of colonies from monoculture samples than compared to the CFU results in **Figure 3.6.1. c)**. Apart from that, dynamically grown *E. coli* bacteria also formed a high count of colonies, demonstrating the advantages of the microfluidic chip. Compared to static conditions, *S. aureus* also showed higher counts of colonies formed in monocultured and polymicrobial samples. These results confirm that a microfluidic chip is a suitable and possibly preferred platform for growing monocultured bacteria and polymicrobial biofilms.

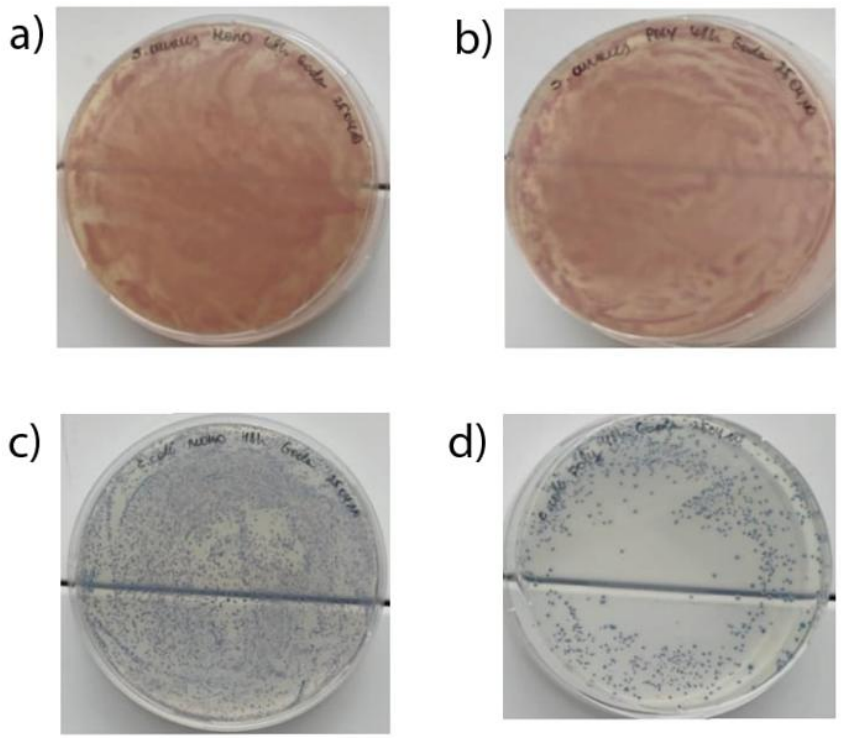

Figure 3.6.2 Results of *S. aureus* and *E. coli* grown under dynamic conditions using microfluidic chip for 48 hours. a) Monoculture *S. aureus* biofilm, shows high count of colonies, b) *S. aureus* collected from a polymicrobial biofilm cultured together with *E. coli*, showing dominant growth of *S. aureus*, c) Monoculture *E. coli* biofilm, exhibiting significantly higher count of colonies then in static conditions, d) *E. coli* from the polymicrobial biofilm, showing high count of colonies.

The experiment was repeated using confocal microscopy analysis to further validate the results gathered from the CFU assay after the growth in a microfluidic system (**Figure 3.6.3.**). It was observed that after 48 hours of growth, the structure of the biofilm was dense, homogenous, and the thickness was 35 µm.

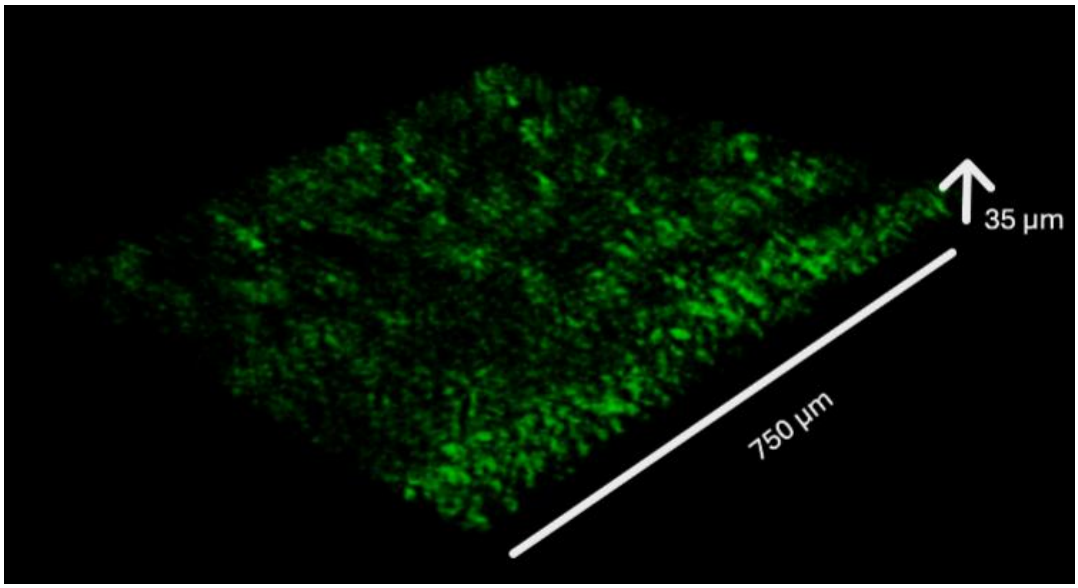

Figure 3.6.3. 3D confocal microscopy image of polymicrobial (*E. coli* and *S. aureus*) biofilm after 48 hours of growth in a microfluidic system.

The presented results confirm that the microfluidic system is a reliable platform for growing and analysing mono– or polymicrobial biofilms under controlled flow. After analysis, it can be concluded that using a microfluidic chip has several advantages, such as biofilms, which can be harder to cultivate using static methods, grow better and more even biofilms in a microfluidic chip. Apart from that, controlled conditions have several benefits, such as minimizing human mistakes, thus moving forward towards more automated and precise results, which is especially important in clinical settings.

4. DISCUSSION

Bacterial biofilms pose a global health threat, allowing them to grow and survive under extreme conditions. In the human body, bacterial biofilms form in the urinary tract, heart valves, or lungs, and in medical devices, such as catheters, stents, or other implantable devices (O'May et al., 2009; Ciofu et al., 2015; Darouiche, 2001). Infections caused by biofilms tend to re–occur, increasing bacterial resistance to antibiotics and causing challenging treatment. Therefore, it is important to understand biofilm formation, the factors included in it, and how they could be manipulated to decrease the severity of infection or fully treat it. Another factor to consider is the currently used methods to study biofilm behaviour, growth, and response to antimicrobial treatments. Traditional methods, such as static ones–CFU, growth in cell–well plates, are popular but cannot mimic the natural environment, limiting their effectiveness and accuracy (Klopper et al., 2024). In a clinical setting, microfluidics has gained a lot of attention due to its capability to closely mimic the natural environment and its relatively large capability to manipulate it to be suitable for a specific experimental setting (Straub et al., 2020). Therefore, in this study, we chose to develop a microfluidic chip for biofilm study with the thought that in the future, it could be applied in a clinical setting.

Microfluidic chips have emerged as a reliable technology that closely replicates the natural environment through controlled shear forces, flow, and gradients of nutrients. Currently, the most widely used microfluidics are PDMS–based. Straub et al. (2020) created a PDMS–based microfluidic chip to investigate *E. coli* under flow. The results showed that a microfluidic chip can mimic natural environments and is a suitable technology for studying bacteria's biofilm response to antibiotics, highlighting its applicability for treatment screening in a clinical setting. Tang et al. (2012) also conducted a similar study, where a microfluidic chip was fabricated to study antibiotic resistance in bacterial biofilms. Results showed that sub-inhibitory ciprofloxacin concentrations could be selected for resistant mutants, thus highlighting the use of microfluidic chips in antibiotic–resistant bacteria evolution.

Although PDMS is a popular material for microfluidic chip fabrication, it has a few drawbacks: gas permeability, deforming under pressure, small molecule absorption, and high hydrophobicity (Vivas et al., 2010; Inglis, 2010; Toepke & Beebe, 2006). The last one poses a challenge because bacteria, which are known to be hydrophilic, poorly adhere to such a microchip surface. Hence, through chemical modifications, PDMS can be made to be hydrophilic and enhance cell attachment (Zhou et al., 2012). However, this brings an additional step to the microfluidic chip fabrication, making it not an ideal solution. Considering the disadvantages, in this work, we chose to produce microfluidic chips using OSTE. OSTE has already been used in the microchip fabrication process and has proven to be a better alternative to PDMS. Amorim et al. (2025) fabricated a microfluidic chip using OSTE polymer and were one of the first scientific groups to test this polymer's

compatibility with bacterial biofilm studies, specifically *S. aureus*. They demonstrated that OSTE–based microfluidic chips are suitable for biofilm studies and have several advantages, such as high mechanical stability and tunable surface chemistry, making them a versatile material to advance biofilm research compared to PDMS or glass–based microchips. Additionally, OSTE use in the microchip fabrication enhances the chip`s durability, in the end reducing experimental costs. Also, it is compatible with COC substrates, which are often used in a laboratory setting, thus creating a pathway for scalable production. Therefore, by using OSTE resin instead of PDMS, we fabricated a microfluidic chip to study biofilms with high accuracy, through enhanced mechanical strength, chemical stability, and high dimensional accuracy.

In this study, we fabricated a microfluidic chip with five independent growth chambers. During the development process, we focused on creating a design that would be applicable in standard laboratory settings. The materials chosen for the chip, apart from being mechanically and chemically stable, also have good optical transparency, enabling clear and accurate visualisation of chambers, flow dynamics, and grown biofilm structure. The enhancements, such as improved master mold design to ease OSTE injection and minimize further leakage, were done to improve and shorten the time of fabrication. Furthermore, the microfluidic chip includes Mini Luer ports and has dimensions that match the standard microscopic slide size, making it more applicable in various laboratory settings, imaging, and evaluation of antimicrobial treatment on biofilms. The incorporation of relatively novel materials and optimized microchip design offers a promising platform for biofilm study, by reducing fabrication and total experimental costs while addressing key limitations in existing platforms.

To create an accurately controlled fluid flow within the microfluidic chips' growth chamber, an important aspect to consider is WSS distribution within it. In this study, the fabricated microchip's WSS were measured, where the highest recorded number was 5.44×10^{-3} Pa near the ends of the growth chamber and the lowest numbers were recorded in the central parts of the chamber, ranging from 1.81×10^{-3} to 3.17×10^{-3} Pa, demonstrating consistent flow. The variations in WSS in different parts of the microfluidic chip were due to the differences in the channel dimensions. Near the inlets and outlets, where the surface area is smaller, WSS was higher than in the center of the channel. Wei & Yang (2023) tested how different flow conditions affect *Pseudomonas putida* biofilm formation in a microfluidic chip. They observed that under consistent 3.5 Pa shear stress with low flow fluctuations, biofilm growth was enhanced, and with high flow fluctuations, the growth was slower or inhibited. These results show the importance of uniform shear stress across the channel because it ensures the reproducibility through minimizing flow stagnation, which is critical for accurate and successful evaluation of biofilm growth and response to antibiotic treatment.

To demonstrate the advantages of microfluidic use for bacterial biofilm analysis, the two bacteria species *S. aureus* and *P. aeruginosa* were grown under dynamic (microfluidic chip) and static (24–well plate) conditions. In both conditions, bacteria were grown for 3, 24, and 48 hours to accurately evaluate the biofilm development in different stages. After 3 hours of growth, biofilms grown in well plates showed heterogeneous and dense adhesion, while under dynamic conditions, early microcolony formation could have been observed. The denser adhesion under static conditions was due to the absence of fluid movement, allowing bacteria to grow exponentially. After 24 hours, the difference in biofilm structures under different conditions was even clearer, where in microchip biofilms were forming uniform layers, and in well plates, the biofilm was continuing to form dense and uneven biofilm layers. At 48 hours, biofilms grown in static conditions showed even more clumped and dense growth vertically, especially for *S. aureus*. Due to consistent and controlled flow, bacteria in the microfluidic chip continued to form an evenly distributed and thin layer of biofilm, restricting the excess biofilm growth, displaying the importance and advantage of shear force in biofilm formation. Tran et al. (2022) compared biofilm formation of S. aureus and Candida albicans under static conditions in 96–well plates and dynamic conditions in microfluidic channels. The results showed that under dynamic conditions, biofilms formed more heterogeneously with higher rates of aggregation and were thicker compared to dynamic conditions where bacteria formed a more even and uniform layer of biofilms, due to shear stress and constant nutrient supply. Although, microfluidic chips for bacterial growth and study are quite a novel approach, it has already been proven as a favourable technology to grow and analyse bacterial biofilm formation, compared to traditional static methods, as it allows to grow evenly distributed biofilms while closely mimic the natural environment due to shear force and controlled flow conditions.

To further evaluate the microfluidic chips' applicability in a clinical setting, bacterial biofilms were treated with ciprofloxacin and tetracycline, a commonly used antibiotics, to assess the fabricated chip's potential for studying biofilm response to antimicrobial treatment. *P. aeruginosa* and *S. aureus* bacteria were grown in a microfluidic chip and treated with ciprofloxacin for 16 hours at a 5 µg/mL flow rate, after which the thickness of biofilm greatly reduced, and the architecture, as seen in confocal images, was disrupted with increased visualisation of dead cells. Additionally, *S. aureus* biofilms grown for 48 hours were treated with increasing concentrations of tetracycline (32, 64, and 128 µg/mL), at a 5 µg/mL flow rate for 16 hours. It was observed that the increase in antibiotic concentration resulted in significant biofilm disruption after treatment, ultimately reducing the bacteria's biofilm from approximately 33 µm to 6 µm. These results confirm the potential of microfluidic chip capability to mimic experimentally needed environments, thus creating a platform for studying the efficacy of antimicrobial treatments *in situ*. It is important to note that during the treatment, *S. aureus* biofilm reduced relatively more compared to *P. aeruginosa*, which may be

because of the differences in biofilm structure and extracellular polymeric substance (EPS) composition variations between the two bacterial species. Vestweber et al. (2024) assessed the morphological differences of both bacterial biofilms, showing that after 48 to 72 hours of growth, *S. aureus* formed a less dense biofilm structure with porous aggregates, while *P. aeruginosa* formed a highly dense and compact biofilm structure. Therefore, the differences in biofilm structure could have influenced the different responses to the treatment. Nevertheless, this pilot experiment demonstrated the microchips' potential to study the effects of antimicrobial efficacy under controlled conditions. However, future research is needed to further validate these results.

In natural environments, bacteria often form polymicrobial biofilms and cause various chronic infections, which are challenging to treat. To test the microfluidic chip's capabilities, we cultivated PMBF consisting of *E. coli* and *S. aureus* bacteria in the channels of the chip. Firstly, we assessed polymicrobial biofilm formation under static conditions using the CFU assay. However, after several attempts, the monocultured *E. coli* and polymicrobial biofilm did not form. This could have happened because *E. coli* is known to detach from the surface more easily than *S. aureus* due to harsh washing with PBS (Zhou et al., 2022). After unsuccessful attempts to grow PMBF under static conditions, bacterial biofilm growth was tested in the microfluidic chip. After the removal of bacteria from the channels using trypsin, they were seeded on the selective agar plates. The results were promising, *E. coli* formed a high count of colonies from monocultivated and PMBF samples. However, the presented results should be repeated in future works to assess the best dilution factor when collecting cells from the growth chamber and seeding them on agar plates. To further analyse the PMBFs' architecture, the experiment was repeated where channels were dyed and analysed using confocal scanning microscopy. The 3D biofilm visualisation showed a 35 µm–thick, dense and evenly distributed biofilm, confirming the results after chemical detachment. Subramanian et al. (2016) investigated the efficacy of the novel treatment against *E. coli* biofilms in the microfluidic device. During the study, they assessed that the average thickness of mature *E. coli* biofilm ranges from 10 µm to 30 µm, therefore, we can say that in our study, we managed to grow PMBFs in the chip. However, we recognise that in future studies, bacteria morphology should be analysed using SEM or a more defined lens of a confocal microscope. These initial results prove that the microfluidic chip is a promising technology with capabilities to ease the study of PMBFs under controlled flow, by minimizing human error and introducing controlled conditions for the most reliable results.

.

.

CONCLUSIONS

1. A microfluidic chip featuring five independent microchannels was successfully fabricated using soft lithography and photolithography techniques. The fabrication process was optimized to ensure high reproducibility and quality, with dimensional variations within ±3%. The device demonstrated no leakage and is cost-effective for further experimental applications.
2. The comparison of dynamic (microfluidic chip) and static (24–well plate) growth conditions of *S. aureus* and *P. aeruginosa* biofilm showed that in the microfluidic chip, a thin and homogenous biofilm layer was formed, while in the well plates, the biofilm was dense and heterogenous.
3. Antimicrobial treatment showed that the fabricated microfluidic chip is a reliable platform for analysing treatment efficacy on bacterial biofilms using confocal scanning microscopy.
4. Polymicrobial biofilm growth consisting of *E. coli* and *S. aureus* was unsuccessful under static conditions, while in the microfluidic chip, it formed a dense and evenly distributed polymicrobial biofilm, confirmed by CFU assay and confocal microscopy analysis.

VILNIUS UNIVERSITY
LIFE SCIENCE CENTER

Goda Grigorianaitė

Master's Thesis

Development of a Microfluidic System for Cultivating and Studying Microbial Biofilms Under Controlled Flow Conditions

ABSTRACT

Microbial biofilms are a group of microorganisms that are embedded in an extracellular polymeric matrix (EPS) and live in a coordinated manner. They cause challenging–to–treat chronic infections or complications related to implantable medical devices, such as urinary catheters, due to their increasing resistance to antibiotics. Recognising this critical issue in the medical field, traditional biofilm study methods often fail to accurately replicate the natural conditions, such as fluid flow, that play a crucial role in biofilm formation.

Recognising current limitations in biofilm study, a microfluidic chip, using off–stoichiometry thiol–ene (OSTE) resin and cyclic olefin copolymer (COC) substrates, was created. The chip consisted of five independent growth chambers, enabling the simultaneous growth of several species of bacteria in one run under controlled fluid flow. The fabricated microfluidic chip is compatible with standard laboratory workflows, enabling real–time analysis and offering a user–friendly approach.

To further emphasize the benefits of the fabricated chip's capabilities to study biofilm, the growth of *Pseudomonas aeruginosa* and *Staphylococcus aureus* was compared under static (24–well plate) and dynamic conditions (microfluidic chip). Analysis using confocal laser scanning microscopy revealed that under static conditions, biofilms were thicker, uneven with heterogeneous structures, while under dynamic conditions, biofilms were more uniformly distributed and thinner. To demonstrate the chip's capability for evaluating antibiotic efficacy, a treatment with ciprofloxacin at 5 μg/mL and different concentrations of tetracycline was performed, leading to significantly reduced biofilm and viability. Additionally, polymicrobial biofilm, consisting of *Escherichia coli* and *Staphylococcus aureus*, was cultivated under static and dynamic conditions. While polymicrobial biofilm did not form under static conditions, it successfully grew under dynamic conditions. Apart from that, to confirm the chip's capability to accurately mimic experimentally relevant fluid flow, computational simulations of wall shear stress were performed.

These results highlight the microfluidic platform’s capabilities to advance biofilm research as a cost–effective, scalable, and reliable tool in a clinical setting.

VILNIAUS UNIVERSITETO
GYBYBĖS MOKSLŲ CENTRAS

Goda Grigorianaitė

Magistro baigiamasis darbas

Mikrofluidinės sistemos kūrimas, skirtos mikrobinių bioplėvelių auginimui ir tyrimui kontroliuojamomis srauto sąlygomis

SANTRAUKA

Bakterijų bioplėvelės – tai mikroorganizmų grupės, apsuptos ekstraląstelinės polimerinės matricos (EPS), kuriose bakterijos gyvena koordinuotai. Dėl didėjančio bakterijų atsparumo antibiotikams, jų suformuotos bioplėvelės dažnai sukelia sunkiai gydomas lėtines infekcijas arba komplikacijas, susijusias su implantuojamais medicinos prietaisais, pavyzdžiui, šlapimo kateteriais. Dėl šios priežasties, tiriant bakterines bioplėveles, yra itin svarbu atkartoti natūralias aplinkos sąlygas, ko dažnu atveju nepavyksta pasiekti naudojant tradicinius tyrimų metodus, pavyzdžiui, skysčių srautą, kuris yra vienas iš svarbesnių aspektų bioplėvelės formavimesi.

Atsižvelgiant į dabartinius bakterinių bioplėvelių tyrimo trūkumus, buvo sukurtas mikrofluidinis lustas, kuriame buvo panaudoti nestechiometrinės tioleno dervos (OSTE) ir ciklinių olefinų kopolimerų (COC) substratai. Mikrofluidinį lustą sudarė penkios nepriklausomos augimo kameros, leidžiančios vienu metu auginti kelių rūšių bakterijas, esant kontroliuojamam skysčio srautui. Taip pat, pagaminta mikrofluidinė sistema yra suderinama su standartiniais laboratoriniais prietaisais, todėl ją galima analizuoti realiu laiku ir ji yra patogi vartotojui.

Siekiant įrodyti pagamintos mikrofluidinės sistemos privalumus tiriant bioplėveles, *Pseudomonas aeruginosa* ir *Staphylococcus aureus* (*S. aureus*) bakterijų augimas buvo lyginamas statinėmis (24 šulinėlių lėkštelėje) ir dinaminėmis sąlygomis (mikrofluidinėje sistemoje). Lazerinė, skenuojančio konfokalinio mikroskopo analizė parodė, kad šulinėliuose bioplėvelės buvo storesnės, nelygios ir nevienalytės struktūros, o dinaminėmis sąlygomis bioplėvelės buvo tolygiau pasiskirsčiusios ir plonesnės. Siekiant įvertinti lusto patikimumą tiriant antibiotikų veiksmingumą, bioplėvelės buvo paveiktos su 5 μg/ml ciprofloksacino ir skirtingomis koncentracijomis tetraciklino, po kurių bioplėvelės storis ir gyvybingumas reikšmingai sumažėjo. Taip pat buvo ištirtas polimikrobinės bioplėvelės augimas (*Escherichia coli* ir *S. aureus*) statinėmis ir dinaminėmis sąlygomis. Statinėmis sąlygomis polimikrobinė bioplėvelė nesusiformavo, tačiau ji sėkmingai augo mikrofluidinėje sistemoje. Siekiant įvertinti mikrofluidinės sistemos galimybes tiksliai imituoti eksperimentinį skysčio tekėjimą, buvo atliktas sienelių šlyties įtempių kompiuterinis modeliavimas.

Šie rezultatai patvirtina mikrofluidinės platformos pritaikomumą klinikinėje aplinkoje kaip ekonomiškai efektyvaus ir patikimo įrankio bakterinės bioplėvelės tyrimams.

ACKNOWLEDGMENTS

I would like to thank my work supervisor, Dr. Wanessa Melo, for the help with the experiments, consultation, shared knowledge, and guidance during the experimentation. Also, I would like to thank Adei Abouhagger for the immense help and guidance during the whole master thesis project with the microfluidic chip fabrication and analysis, and for always encouraging and pushing forward.

REFERENCES

Abedon, S. T., Duffy, S., & Turner, P. E. (2009). Bacteriophage Ecology. In *Encyclopedia of Microbiology* (pp. 42–57). Elsevier. https://doi.org/10.1016/B978–012373944–5.00022–5

Adamiak, W., Kałuża, D., & Jönsson–Niedziolka, M. (2016). Compatibility of organic solvents for electrochemical measurements in PDMS–based microfluidic devices. *Microfluidics and Nanofluidics*, *20*(9), 127. https://doi.org/10.1007/s10404–016–1792–4

Alcàcer–Almansa, J., Arévalo–Jaimes, B. V., Blanco–Cabra, N., & Torrents, E. (2023). Methods for studying biofilms: Microfluidics and translation in the clinical context. In *Methods in Microbiology* (Vol. 53, pp. 195–233). Elsevier. https://doi.org/10.1016/bs.mim.2023.04.002

Alves, P. M., Al–Badi, E., Withycombe, C., Jones, P. M., Purdy, K. J., & Maddocks, S. E. (2018a). Interaction between Staphylococcus aureus and Pseudomonas aeruginosa is beneficial for colonisation and pathogenicity in a mixed biofilm. *Pathogens and Disease*, *76*(1). https://doi.org/10.1093/femspd/fty003

Alves, P. M., Al–Badi, E., Withycombe, C., Jones, P. M., Purdy, K. J., & Maddocks, S. E. (2018b). Interaction between Staphylococcus aureus and Pseudomonas aeruginosa is beneficial for colonisation and pathogenicity in a mixed biofilm. *Pathogens and Disease*, *76*(1). https://doi.org/10.1093/femspd/fty003

Amorim, J., Rosqvist, E., Cruz, C. D., Haapala, M., Peltonen, J., Tammela, P., & Sikanen, T. M. (2025). A Systematic Study of *Staphylococcus aureus* Biofilm Formation on Thiol-Ene Polymers: Toward the Development of Microfluidic Bacterial Biofilm Models. *Advanced Materials Interfaces*, 2400910. https://doi.org/10.1002/admi.202400910

Anju, V. T., Busi, S., Imchen, M., Kumavath, R., Mohan, M. S., Salim, S. A., Subhaswaraj, P., & Dyavaiah, M. (2022). Polymicrobial Infections and Biofilms: Clinical Significance and Eradication Strategies. *Antibiotics (Basel, Switzerland)*, *11*(12), 1731. https://doi.org/10.3390/antibiotics11121731

Arunachalam, K., & Davoodbasha, M. (2021). Imaging Bacteria and Biofilm by Field Emission Scanning Electron Microscopy. In M. Nag & D. Lahiri (Eds.), *Analytical Methodologies for Biofilm Research* (pp. 205–222). Springer US. https://doi.org/10.1007/978–1–0716–1378–8_9

Azeredo, J., Azevedo, N. F., Briandet, R., Cerca, N., Coenye, T., Costa, A. R., Desvaux, M., Di Bonaventura, G., Hébraud, M., Jaglic, Z., Kačániová, M., Knøchel, S., Lourenço, A., Mergulhão, F., Meyer, R. L., Nychas, G., Simões, M., Tresse, O., & Sternberg, C. (2017). Critical review on biofilm methods. *Critical Reviews in Microbiology*, *43*(3), 313–351. https://doi.org/10.1080/1040841X.2016.1208146

Ballén, V., Cepas, V., Ratia, C., Gabasa, Y., & Soto, S. M. (2022). Clinical Escherichia coli: From Biofilm Formation to New Antibiofilm Strategies. *Microorganisms*, *10*(6), 1103. https://doi.org/10.3390/microorganisms10061103

Bruijns, B., Veciana, A., Tiggelaar, R., & Gardeniers, H. (2019). Cyclic Olefin Copolymer Microfluidic Devices for Forensic Applications. *Biosensors*, *9*(3), 85. https://doi.org/10.3390/bios9030085

Buckingham–Meyer, K., Goeres, D. M., & Hamilton, M. A. (2007). Comparative evaluation of biofilm disinfectant efficacy tests. *Journal of Microbiological Methods*, *70*(2), 236–244. https://doi.org/10.1016/j.mimet.2007.04.010

Campbell, S. B., Wu, Q., Yazbeck, J., Liu, C., Okhovatian, S., & Radisic, M. (2021). Beyond Polydimethylsiloxane: Alternative Materials for Fabrication of Organ–on–a–Chip Devices and Microphysiological Systems. *ACS Biomaterials Science & Engineering*, *7*(7), 2880–2899. https://doi.org/10.1021/acsbiomaterials.0c00640

Camus, L., Briaud, P., Vandenesch, F., Doléans–Jordheim, A., & Moreau, K. (2022). Mixed Populations and Co–Infection: Pseudomonas aeruginosa and Staphylococcus aureus. In A. Filloux & J.–L. Ramos (Eds.), *Pseudomonas aeruginosa* (Vol. 1386, pp. 397–424). Springer International Publishing. https://doi.org/10.1007/978–3–031–08491–1_15

Carlborg, C. F., Haraldsson, T., Öberg, K., Malkoch, M., & Van Der Wijngaart, W. (2011). Beyond PDMS: Off–stoichiometry thiol–ene (OSTE) based soft lithography for rapid prototyping of microfluidic devices. *Lab on a Chip*, *11*(18), 3136. https://doi.org/10.1039/c1lc20388f

Cattò, C., & Cappitelli, F. (2019). Testing Anti–Biofilm Polymeric Surfaces: Where to Start? *International Journal of Molecular Sciences*, *20*(15), 3794. https://doi.org/10.3390/ijms20153794

Chandki, R., Banthia, P., & Banthia, R. (2011). Biofilms: A microbial home. *Journal of Indian Society of Periodontology*, *15*(2), 111–114. https://doi.org/10.4103/0972–124X.84377

Cheah, H., & Bae, S. (2023). Multichannel Microfluidic Platform for Temporal–Spatial Investigation of Niche Roles of Pseudomonas aeruginosa and Escherichia coli within a Dual–Species Biofilm. *Applied and Environmental Microbiology*, *89*(7), e00651–23. https://doi.org/10.1128/aem.00651–23

Ciofu, O., Tolker–Nielsen, T., Jensen, P. Ø., Wang, H., & Høiby, N. (2015). Antimicrobial resistance, respiratory tract infections and role of biofilms in lung infections in cystic fibrosis patients. *Advanced Drug Delivery Reviews*, *85*, 7–23. https://doi.org/10.1016/j.addr.2014.11.017

Cleaver, L., & Garnett, J. A. (2023). How to study biofilms: Technological advancements in clinical biofilm research. *Frontiers in Cellular and Infection Microbiology*, *13*, 1335389. https://doi.org/10.3389/fcimb.2023.1335389

Coenye, T., & Nelis, H. J. (2010). In vitro and in vivo model systems to study microbial biofilm formation. *Journal of Microbiological Methods*, *83*(2), 89–105. https://doi.org/10.1016/j.mimet.2010.08.018

Colin, V. G., Travers, T., Gindre, D., Barillé, R., & Loumaigne, M. (2021). Cheap, versatile, and turnkey fabrication of microfluidic master molds using consumer–grade LCD stereolithography 3D printing. *The International Journal of Advanced Manufacturing Technology*, *116*(1–2), 537–544. https://doi.org/10.1007/s00170–021–07329–3

Crivello, G., Fracchia, L., Ciardelli, G., Boffito, M., & Mattu, C. (2023). In Vitro Models of Bacterial Biofilms: Innovative Tools to Improve Understanding and Treatment of Infections. *Nanomaterials*, *13*(5), 904. https://doi.org/10.3390/nano13050904

Darouiche, R. O. (2001). Device-Associated Infections: A Macroproblem that Starts with Microadherence. *Clinical Infectious Diseases*, *33*(9), 1567–1572. https://doi.org/10.1086/323130

Dhiman, S., Kumar, A., Kaur, G., Mukherjee, G., Rustagi, S., Shreaz, S., Negi, R., & Yadav, A. N. (2024). Bacterial biofilms: Pathogenesis, monitoring, treatment approaches and associated challenges. *Biologia*, *79*(10), 3161–3181. https://doi.org/10.1007/s11756–024–01767–6

Fernández–la–Villa, A., Pozo–Ayuso, D. F., & Castaño–Álvarez, M. (2019). Microfluidics and electrochemistry: An emerging tandem for next–generation analytical microsystems. *Current Opinion in Electrochemistry*, *15*, 175–185. https://doi.org/10.1016/j.coelec.2019.05.014

Fleming, D., & Rumbaugh, K. P. (2017). Approaches to Dispersing Medical Biofilms. *Microorganisms*, *5*(2), 15. https://doi.org/10.3390/microorganisms5020015

Focaroli, S., Mazzitelli, S., Falconi, M., Luca, G., & Nastruzzi, C. (2014). Preparation and validation of low cost microfluidic chips using a shrinking approach. *Lab Chip*, *14*(20), 4007–4016. https://doi.org/10.1039/C4LC00679H

Gupta, P., Sarkar, S., Das, B., Bhattacharjee, S., & Tribedi, P. (2016). Biofilm, pathogenesis and prevention—a journey to break the wall: A review. *Archives of Microbiology*, *198*(1), 1–15. https://doi.org/10.1007/s00203–015–1148–6

Hardy, B. S., Uechi, K., Zhen, J., & Pirouz Kavehpour, H. (2009). The deformation of flexible PDMS microchannels under a pressure driven flow. *Lab Chip*, *9*(7), 935–938. https://doi.org/10.1039/B813061B

Hwang, J., Cho, Y. H., Park, M. S., & Kim, B. H. (2019). Microchannel Fabrication on Glass Materials for Microfluidic Devices. *International Journal of Precision Engineering and Manufacturing*, *20*(3), 479–495. https://doi.org/10.1007/s12541–019–00103–2

Inglis, D. W. (2010). A method for reducing pressure–induced deformation in silicone microfluidics. *Biomicrofluidics*, *4*(2), 026504. https://doi.org/10.1063/1.3431715

Jamal, M., Ahmad, W., Andleeb, S., Jalil, F., Imran, M., Nawaz, M. A., Hussain, T., Ali, M., Rafiq, M., & Kamil, M. A. (2018). Bacterial biofilm and associated infections. *Journal of the Chinese Medical Association*, *81*(1), 7–11. https://doi.org/10.1016/j.jcma.2017.07.012

Keown, K., Reid, A., Moore, J. E., Taggart, C. C., & Downey, D. G. (2020). Coinfection with *Pseudomonas aeruginosa* and *Aspergillus fumigatus* in cystic fibrosis. *European Respiratory Review*, *29*(158), 200011. https://doi.org/10.1183/16000617.0011–2020

Kim, J., Park, H.–D., & Chung, S. (2012). Microfluidic Approaches to Bacterial Biofilm Formation. *Molecules*, *17*(8), 9818–9834. https://doi.org/10.3390/molecules17089818

Klopper, K. B., Bester, E., Van Schalkwyk, M., & Wolfaardt, G. M. (2024). Highlighting the limitations of static microplate biofilm assays for industrial biocide effectiveness compared to dynamic flow conditions. *Environmental Microbiology Reports*, *16*(1), e13214. https://doi.org/10.1111/1758–2229.13214

Kong, E. F., Tsui, C., Kucharíková, S., Andes, D., Van Dijck, P., & Jabra–Rizk, M. A. (2016). Commensal Protection of Staphylococcus aureus against Antimicrobials by Candida albicans Biofilm Matrix. *mBio*, *7*(5), e01365–16. https://doi.org/10.1128/mBio.01365–16

Kotz, F., Helmer, D., & Rapp, B. E. (2020). Emerging Technologies and Materials for High–Resolution 3D Printing of Microfluidic Chips. In J. Bahnemann & A. Grünberger (Eds.), *Microfluidics in Biotechnology* (Vol. 179, pp. 37–66). Springer International Publishing. https://doi.org/10.1007/10_2020_141

Lai, X., Lu, B., Zhang, P., Zhang, X., Pu, Z., Yu, H., & Li, D. (2019). Sticker Microfluidics: A Method for Fabrication of Customized Monolithic Microfluidics. *ACS Biomaterials Science & Engineering*, *5*(12), 6801–6810. https://doi.org/10.1021/acsbiomaterials.9b00953

Li, L., Mendis, N., Trigui, H., Oliver, J. D., & Faucher, S. P. (2014). The importance of the viable but non–culturable state in human bacterial pathogens. *Frontiers in Microbiology*, *5*. https://doi.org/10.3389/fmicb.2014.00258

Lobo, C. I. V., Rinaldi, T. B., Christiano, C. M. S., De Sales Leite, L., Barbugli, P. A., & Klein, M. I. (2019). Dual–species biofilms of *Streptococcus mutans* and *Candida albicans* exhibit more biomass and are mutually beneficial compared with single–species biofilms. *Journal of Oral Microbiology*, *11*(1), 1581520. https://doi.org/10.1080/20002297.2019.1581520

Ma, R., Hu, X., Zhang, X., Wang, W., Sun, J., Su, Z., & Zhu, C. (2022). Strategies to prevent, curb and eliminate biofilm formation based on the characteristics of various periods in one biofilm life cycle. *Frontiers in Cellular and Infection Microbiology*, *12*, 1003033. https://doi.org/10.3389/fcimb.2022.1003033

Manz, W., Szewzyk, U., Ericsson, P., Amann, R., Schleifer, K. H., & Stenström, T. A. (1993). In situ identification of bacteria in drinking water and adjoining biofilms by hybridization with 16S

and 23S rRNA–directed fluorescent oligonucleotide probes. *Applied and Environmental Microbiology*, *59*(7), 2293–2298. https://doi.org/10.1128/aem.59.7.2293–2298.1993

Margarida Pereira, A., Cristina Abreu, A., & Simões, M. (2012). Action of Kanamycin Against Single and Dual Species Biofilms of *Escherichia coli and Staphylococcus aureus*. *Journal of Microbiology Research*, *2*(4), 84–88. https://doi.org/10.5923/j.microbiology.20120204.04

Marić, S., & Vraneš, J. (2007). Characteristics and Significance of Microbial Biofilm Formation. *Periodicum Biologorum*, *109*, 115.

McCoy, W. F., Bryers, J. D., Robbins, J., & Costerton, J. W. (1981). Observations of fouling biofilm formation. *Canadian Journal of Microbiology*, *27*(9), 910–917. https://doi.org/10.1139/m81–143

Mitchell, C. J., Hu, T., Sun, S., Stirling, C. J., Nedeljkovic, M., Peacock, A. C., Reed, G. T., Mashanovich, G. Z., & Rowe, D. J. (2024). Mid–infrared silicon photonics: From benchtop to real–world applications. *APL Photonics*, *9*(8), 080901. https://doi.org/10.1063/5.0222890

Mountcastle, S. E., Vyas, N., Villapun, V. M., Cox, S. C., Jabbari, S., Sammons, R. L., Shelton, R. M., Walmsley, A. D., & Kuehne, S. A. (2021). Biofilm viability checker: An open–source tool for automated biofilm viability analysis from confocal microscopy images. *Npj Biofilms and Microbiomes*, *7*(1), 44. https://doi.org/10.1038/s41522–021–00214–7

Nielsen, J. B., Hanson, R. L., Almughamsi, H. M., Pang, C., Fish, T. R., & Woolley, A. T. (2020). Microfluidics: Innovations in Materials and Their Fabrication and Functionalization. *Analytical Chemistry*, *92*(1), 150–168. https://doi.org/10.1021/acs.analchem.9b04986

Ofner, A., Moore, D. G., Rühs, P. A., Schwendimann, P., Eggersdorfer, M., Amstad, E., Weitz, D. A., & Studart, A. R. (2017). High-Throughput Step Emulsification for the Production of Functional Materials Using a Glass Microfluidic Device. *Macromolecular Chemistry and Physics*, *218*(2), 1600472. https://doi.org/10.1002/macp.201600472

O'May, G. A., Jacobsen, S. M., Stickler, D. J., Mobley, H. L. T., & Shirtliff, M. E. (2009). Complicated Urinary Tract Infections due to Catheters. In M. Shirtliff & J. G. Leid (Eds.), *The Role of Biofilms in Device–Related Infections* (Vol. 3, pp. 123–165). Springer Berlin Heidelberg. https://doi.org/10.1007/978–3–540–68119–9_6

O'Toole, G. A. (2011). Microtiter dish biofilm formation assay. *Journal of Visualized Experiments: JoVE*, *47*, 2437. https://doi.org/10.3791/2437

Pan, L.–J., Tu, J.–W., Ma, H.–T., Yang, Y.–J., Tian, Z.–Q., Pang, D.–W., & Zhang, Z.–L. (2018). Controllable synthesis of nanocrystals in droplet reactors. *Lab on a Chip*, *18*(1), 41–56. https://doi.org/10.1039/C7LC00800G

Park, I., Jailani, A., Lee, J.–H., Ahmed, B., & Lee, J. (2023). The Antibiofilm Effects of Antimony Tin Oxide Nanoparticles against Polymicrobial Biofilms of Uropathogenic Escherichia

coli and Staphylococcus aureus. *Pharmaceutics*, *15*(6), 1679. https://doi.org/10.3390/pharmaceutics15061679

Pérez-Rodríguez, S., García-Aznar, J. M., & Gonzalo-Asensio, J. (2022). Microfluidic devices for studying bacterial taxis, drug testing and biofilm formation. *Microbial Biotechnology*, *15*(2), 395–414. https://doi.org/10.1111/1751–7915.13775

Pranzo, D., Larizza, P., Filippini, D., & Percoco, G. (2018). Extrusion–Based 3D Printing of Microfluidic Devices for Chemical and Biomedical Applications: A Topical Review. *Micromachines*, *9*(8), 374. https://doi.org/10.3390/mi9080374

Preda, V. G., & Săndulescu, O. (2019). Communication is the key: Biofilms, quorum sensing, formation and prevention. *Discoveries (Craiova, Romania)*, *7*(3), e100. https://doi.org/10.15190/d.2019.13

Qin, S., Xiao, W., Zhou, C., Pu, Q., Deng, X., Lan, L., Liang, H., Song, X., & Wu, M. (2022). Pseudomonas aeruginosa: Pathogenesis, virulence factors, antibiotic resistance, interaction with host, technology advances and emerging therapeutics. *Signal Transduction and Targeted Therapy*, *7*(1), 199. https://doi.org/10.1038/s41392–022–01056–1

Rather, M. A., Gupta, K., & Mandal, M. (2021). Microbial biofilm: Formation, architecture, antibiotic resistance, and control strategies. *Brazilian Journal of Microbiology*, *52*(4), 1701–1718. https://doi.org/10.1007/s42770–021–00624–x

Richmond, T., & Tompkins, N. (2021). 3D microfluidics in PDMS: Manufacturing with 3D molding. *Microfluidics and Nanofluidics*, *25*(9), 76. https://doi.org/10.1007/s10404–021–02478–z

Rodrigues, C. F., Allkja, J., Mendes, L., & Azevedo, A. S. (2023). Methods for the Visualization of Multispecies Biofilms. In K. S. Kaushik & S. E. Darch (Eds.), *Multispecies Biofilms* (Vol. 12, pp. 35–78). Springer International Publishing. https://doi.org/10.1007/978–3–031–15349–5_2

Sauer, K., Stoodley, P., Goeres, D. M., Hall–Stoodley, L., Burmølle, M., Stewart, P. S., & Bjarnsholt, T. (2022). The biofilm life cycle: Expanding the conceptual model of biofilm formation. *Nature Reviews Microbiology*, *20*(10), 608–620. https://doi.org/10.1038/s41579–022–00767–0

Schulze, A., Mitterer, F., Pombo, J. P., & Schild, S. (n.d.). Biofilms by bacterial human pathogens: Clinical relevance – development, composition and regulation – therapeutical strategies. *Microbial Cell*, *8*(2), 28–56. https://doi.org/10.15698/mic2021.02.741

Schwartz, K., Stephenson, R., Hernandez, M., Jambang, N., & Boles, B. R. (2010a). The use of drip flow and rotating disk reactors for Staphylococcus aureus biofilm analysis. *Journal of Visualized Experiments: JoVE*, *46*, 2470. https://doi.org/10.3791/2470

Schwartz, K., Stephenson, R., Hernandez, M., Jambang, N., & Boles, B. R. (2010b). The use of drip flow and rotating disk reactors for Staphylococcus aureus biofilm analysis. *Journal of Visualized Experiments: JoVE*, *46*, 2470. https://doi.org/10.3791/2470

Shakeri, A., Jarad, N. A., Leung, A., Soleymani, L., & Didar, T. F. (2019). Biofunctionalization of Glass- and Paper-Based Microfluidic Devices: A Review. *Advanced Materials Interfaces*, *6*(19), 1900940. https://doi.org/10.1002/admi.201900940

Sharma, S., Mohler, J., Mahajan, S. D., Schwartz, S. A., Bruggemann, L., & Aalinkeel, R. (2023). Microbial Biofilm: A Review on Formation, Infection, Antibiotic Resistance, Control Measures, and Innovative Treatment. *Microorganisms*, *11*(6), Article 6. https://doi.org/10.3390/microorganisms11061614

Smith, K., Rajendran, R., Kerr, S., Lappin, D. F., Mackay, W. G., Williams, C., & Ramage, G. (2015). *Aspergillus fumigatus* enhances elastase production in *Pseudomonas aeruginosa* co–cultures. *Medical Mycology*, *53*(7), 645–655. https://doi.org/10.1093/mmy/myv048

Son, K., Brumley, D. R., & Stocker, R. (2015). Live from under the lens: Exploring microbial motility with dynamic imaging and microfluidics. *Nature Reviews Microbiology*, *13*(12), 761–775. https://doi.org/10.1038/nrmicro3567

Sticker, D., Geczy, R., Häfeli, U. O., & Kutter, J. P. (2020). Thiol–Ene Based Polymers as Versatile Materials for Microfluidic Devices for Life Sciences Applications. *ACS Applied Materials & Interfaces*, *12*(9), 10080–10095. https://doi.org/10.1021/acsami.9b22050

Straub, H., Eberl, L., Zinn, M., Rossi, R. M., Maniura–Weber, K., & Ren, Q. (2020). A microfluidic platform for in situ investigation of biofilm formation and its treatment under controlled conditions. *Journal of Nanobiotechnology*, *18*(1), 166. https://doi.org/10.1186/s12951–020–00724–0

Subramanian, S., Gerasopoulos, K., Guo, M., Sintim, H. O., Bentley, W. E., & Ghodssi, R. (2016). Autoinducer–2 analogs and electric fields—An antibiotic–free bacterial biofilm combination treatment. *Biomedical Microdevices*, *18*(5). https://doi.org/10.1007/s10544–016–0120–9

Tang, P.–C., Eriksson, O., Sjögren, J., Fatsis–Kavalopoulos, N., Kreuger, J., & Andersson, D. I. (2022). A Microfluidic Chip for Studies of the Dynamics of Antibiotic Resistance Selection in Bacterial Biofilms. *Frontiers in Cellular and Infection Microbiology*, *12*, 896149. https://doi.org/10.3389/fcimb.2022.896149

Teodósio, J. S., Simões, M., Melo, L. F., & Mergulhão, F. J. (2011). Flow cell hydrodynamics and their effects on *E. coli* biofilm formation under different nutrient conditions and turbulent flow. *Biofouling*, *27*(1), 1–11. https://doi.org/10.1080/08927014.2010.535206

Toepke, M. W., & Beebe, D. J. (2006). PDMS absorption of small molecules and consequences in microfluidic applications. *Lab on a Chip*, *6*(12), 1484. https://doi.org/10.1039/b612140c

Tong, S. Y. C., Davis, J. S., Eichenberger, E., Holland, T. L., & Fowler, V. G. (2015). Staphylococcus aureus infections: Epidemiology, pathophysiology, clinical manifestations, and management. *Clinical Microbiology Reviews*, *28*(3), 603–661. https://doi.org/10.1128/CMR.00134–14

Tran, V. N., Khan, F., Han, W., Luluil, M., Truong, V. G., Yun, H. G., Choi, S., Kim, Y.–M., Shin, J. H., & Kang, H. W. (2022a). Real–time monitoring of mono– and dual–species biofilm formation and eradication using microfluidic platform. *Scientific Reports*, *12*(1), 9678. https://doi.org/10.1038/s41598–022–13699–9

Tran, V. N., Khan, F., Han, W., Luluil, M., Truong, V. G., Yun, H. G., Choi, S., Kim, Y.–M., Shin, J. H., & Kang, H. W. (2022b). Real–time monitoring of mono– and dual–species biofilm formation and eradication using microfluidic platform. *Scientific Reports*, *12*(1), 9678. https://doi.org/10.1038/s41598–022–13699–9

Vestweber, P. K., Wächter, J., Planz, V., Jung, N., & Windbergs, M. (2024). The interplay of Pseudomonas aeruginosa and Staphylococcus aureus in dual–species biofilms impacts development, antibiotic resistance and virulence of biofilms in in vitro wound infection models. *PLOS ONE*, *19*(5), e0304491. https://doi.org/10.1371/journal.pone.0304491

Vivas, E. L., Beltran, A. B., Cascon, H. R., Ahn, J., Cho, E. S., & Chung, W. J. (2010). Inorganic filler selection in PDMS membrane for acetone recovery and its application in a condenser–gas membrane system. *Desalination and Water Treatment*, *17*(1–3), 160–167. https://doi.org/10.5004/dwt.2010.1713

Wang, Z., Martin, N., Hini, D., Mills, B., & Kim, K. (2017). Rapid Fabrication of Multilayer Microfluidic Devices Using the Liquid Crystal Display–Based Stereolithography 3D Printing System. *3D Printing and Additive Manufacturing*, *4*(3), 156–164. https://doi.org/10.1089/3dp.2017.0028

Wei, G., & Yang, J. Q. (2023a). Microfluidic investigation of the impacts of flow fluctuations on the development of Pseudomonas putida biofilms. *Npj Biofilms and Microbiomes*, *9*(1), 73. https://doi.org/10.1038/s41522–023–00442–z

Wei, G., & Yang, J. Q. (2023b). Microfluidic investigation of the impacts of flow fluctuations on the development of Pseudomonas putida biofilms. *Npj Biofilms and Microbiomes*, *9*(1), 73. https://doi.org/10.1038/s41522–023–00442–z

Wei, T., Tang, Z., Yu, Q., & Chen, H. (2017). Smart Antibacterial Surfaces with Switchable Bacteria–Killing and Bacteria–Releasing Capabilities. *ACS Applied Materials & Interfaces*, *9*(43), 37511–37523. https://doi.org/10.1021/acsami.7b13565

Wong, I., & Ho, C.–M. (2009). Surface molecular property modifications for poly(dimethylsiloxane) (PDMS) based microfluidic devices. *Microfluidics and Nanofluidics*, *7*(3), 291. https://doi.org/10.1007/s10404–009–0443–4

Xi, C., Marks, D., Schlachter, S., Luo, W., & Boppart, S. A. (2006). High–resolution three–dimensional imaging of biofilm development using optical coherence tomography. *Journal of Biomedical Optics*, *11*(3), 034001. https://doi.org/10.1117/1.2209962

Yuan, L., De Haan, P., Peterson, B. W., De Jong, E. D., Verpoorte, E., Van Der Mei, H. C., & Busscher, H. J. (2020). Visualization of Bacterial Colonization and Cellular Layers in a Gut–on–a–Chip System Using Optical Coherence Tomography. *Microscopy and Microanalysis*, *26*(6), 1211–1219. https://doi.org/10.1017/S143192762002454X

Yuan, L., Straub, H., Shishaeva, L., & Ren, Q. (2023). Microfluidics for Biofilm Studies. *Annual Review of Analytical Chemistry*, *16*(1), 139–159. https://doi.org/10.1146/annurev–anchem–091522–103827

Zheng, S., Bawazir, M., Dhall, A., Kim, H.–E., He, L., Heo, J., & Hwang, G. (2021). Implication of Surface Properties, Bacterial Motility, and Hydrodynamic Conditions on Bacterial Surface Sensing and Their Initial Adhesion. *Frontiers in Bioengineering and Biotechnology*, *9*, 643722. https://doi.org/10.3389/fbioe.2021.643722

Zhou, F., Wang, D., Hu, J., Zhang, Y., Tan, B. K., & Lin, S. (2022). Control Measurements of Escherichia coli Biofilm: A Review. *Foods*, *11*(16), 2469. https://doi.org/10.3390/foods11162469

Zhou, J., Khodakov, D. A., Ellis, A. V., & Voelcker, N. H. (2012). Surface modification for PDMS-based microfluidic devices. *ELECTROPHORESIS*, *33*(1), 89–104. https://doi.org/10.1002/elps.201100482

Zou, Y., Lu, K., Lin, Y., Wu, Y., Wang, Y., Li, L., Huang, C., Zhang, Y., Brash, J. L., Chen, H., & Yu, Q. (2021). Dual–Functional Surfaces Based on an Antifouling Polymer and a Natural Antibiofilm Molecule: Prevention of Biofilm Formation without Using Biocides. *ACS Applied Materials & Interfaces*, *13*(38), 45191–45200. https://doi.org/10.1021/acsami.1c10747

SUPPLEMENTARY

In this work, artificial intelligence tools, such as grammarly.com, were used to edit and improve text fluency.